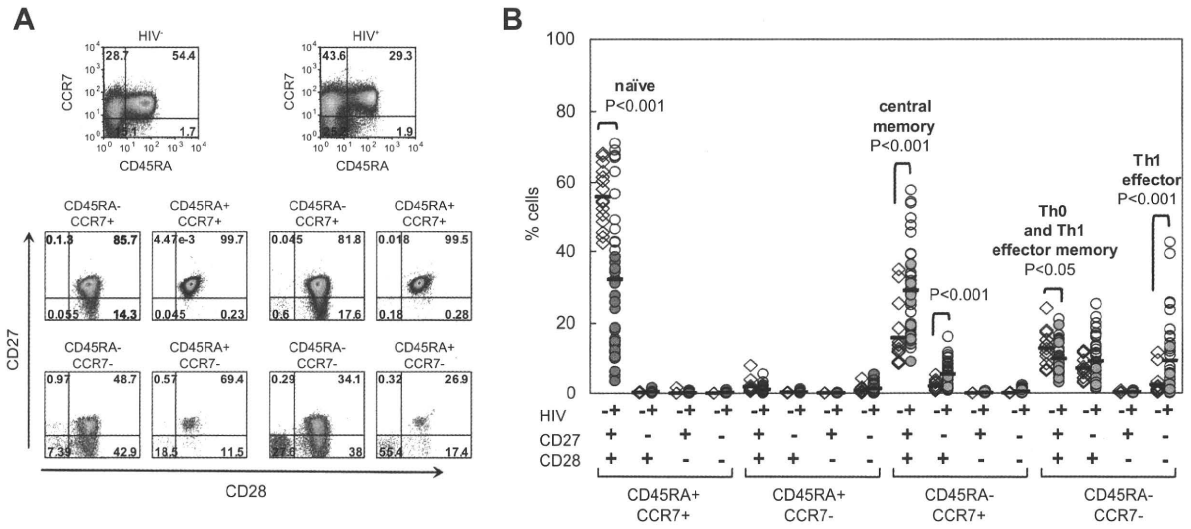

Fig. 1. Phenotypic definition of $CD4^+$ T cells. (A) Flow cytometric analysis of peripheral $CD4^+$ T cells from HIV^- and HIV^+ PBMCs. Live $CD4^+$ lymphocytes were gated and analyzed for CD45RA and CCR7 expression. Each subset was further divided into functionally distinct subpopulations based on the expression of CD27 and CD28. (B) $CD4^+$ T-cell-population distribution in HIV^- and HIV^+ PBMCs. Peripheral $CD4^+$ T cells were phenotypically defined as described in (A). Diamonds and circles indicate peripheral $CD4^+$ T cells from HIV^- individuals and chronically infected patients, respectively. Shaded circles represent patients' $CD4^+$ T cells that were two standard deviations below the mean of uninfected samples in the naïve population, and open circles indicate patient samples which stayed within two standard deviations from the mean of the uninfected control group in the naïve subset. All of the HIV^+ subjects were aviremic, who were in the chronic phase of HIV-1 infection and treated with ART. $CD45RA^+CCR7^+CD27^+CD28^+$ and $CD45RA^-CCR7^+CD27^+CD28^+$ subsets contain naïve and central memory cells, respectively. Th0 and Th1 effector memory cells are found in the $CD45RA^-CCR7^-CD27^-CD28^-$ subset whereas $CD45RA^-CCR7^-CD27^-CD28^-$ cells are predominantly Th1 effector. p-Values were determined in comparison with the uninfected individuals, using Student's t-test.

collection, ranging from 87 to 970 cells/μl with a mean of 479 (median 493) in the <2SD group and 340 to 950 cells/μl with a mean of 499 (median 464) in the w/i 2SD group (Fig. 2A). However, nadir CD4 counts were significantly lower in the <2SD group. The mean CD4 nadir was 82 cells/μl in the HIV^+ < 2SD population (5–342 cells/μl, median 44 cells/μl) whereas the w/i 2SD group maintained 63–312 $CD4^+$ T cells/μl (mean 192 and median 210 cells/μl, $p < 0.005$, Fig. 2A). The majority of the HIV^+ < 2SD individuals had nadir CD4 counts less than 150 cells/μl, suggesting that patients with low CD4 nadir tend to have severely imbalanced CD4 subsets. We also investigated whether the frequency of the naïve subset was dependent on the time of $CD4^+$ T-cell recovery. We did not see a correlation between the severity of naïve-subset depletion and various time elements, including time elapsed since diagnosis till nadir and nadir till sample collection (data not shown). Furthermore, neither the age at the start of ART nor the duration of ART predicted the frequency of naïve subset (Supplementary Table 1). These observations suggested that nadir CD4 counts had a significant impact on the loss of the naïve subset in aviremic HIV^+ patients treated with ART.

3.3. Functional CD4 subsets showed a significantly skewed distribution in patients with low baseline CD4 counts

To investigate the effect of nadir CD4 counts on the imbalanced distribution of functional subsets, we divided HIV^+ patients into five groups based on their nadir CD4 counts; (1) less than 50 cells/μl, (2) 50–100 cells/μl, (3) 100–150 cells/μl, (4) 150–250 cells/μl, and (5) above 250 cells/μl. The five groups did not have a statistical difference in their average CD4 counts at the time of sampling: mean/median CD4 counts for Group 1 = 446/388, Group 2 = 428/407, Group 3 = 453/503, Group 4 = 554/624, and Group 5 = 502/630 cells/μl (Supplementary Table 1). However, the CD4 subset distribution was considerably different. In the groups which had less than 50 and 50–100 cells/μl of nadir CD4 counts (Groups 1 and 2), only 17.6% and 28.2% of the $CD4^+$ T cells were naïve, respectively, as opposed to 38.–46.7% in the rest of the five groups and 55.8% in the uninfected individuals (Fig. 2B). A concomitant increase was detected in the effector subset, which accounted for 14.3% and 15.3% in Groups 1 and 2, respectively. Groups 3–5 had 3.7–5.9% of effector cells and the uninfected control subjects had 2.5% (Fig. 2B). When compared with uninfected individuals, the fractions of three subsets, naïve, T_{CM}, and effector, showed significantly skewed distributions in chronic patients with nadir CD4 counts less than 100 cells/μl (Fig. 2B). These observations suggested that low nadir CD4 was closely associated with a persisting and severely skewed distribution of the CD4 functional subsets, and CD4 nadir, rather than current CD4 counts, had a significant impact on the CD4-subset distribution even though the patients were aviremic because of ART.

3.4. Imbalanced distribution of peripheral $CD4^+$ T-cell subsets persisted for years in HIV^+ patients with low nadir CD4 counts

To investigate the magnitude of subset imbalance and the recovery of a normal distribution as CD4 counts increased

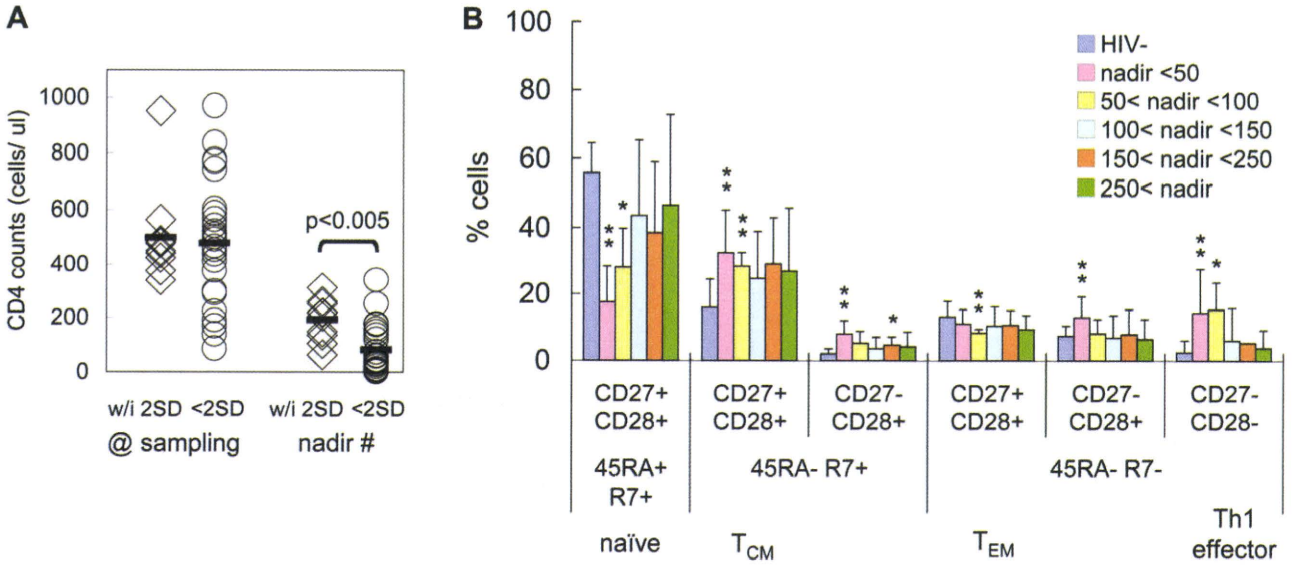

Fig. 2. Factors affecting the frequency of the naïve CD4 T-cell subset. (A) Peripheral $CD4^+$ T-cell counts in 34 patients. The *y*-axis indicates CD4 counts (cells/μl) at the time of sample collection (at sampling) and CD4 nadir in each patient (nadir #). w/i 2SD (diamonds) represents HIV^+ patients whose naïve $CD4^+$ T-cell number falls within two standard deviations of the mean of uninfected samples as indicated in open circles in Fig. 1B; <2SD (circles) shows HIV^+ patient samples that were more than two standard deviations away from the mean of naïve $CD4^+$ cells in uninfected individuals (shaded circles in Fig. 1B). (B) Impact of nadir CD4 counts on $CD4^+$ T-cell subset distribution. The frequencies of $CD4^+$ T-cell subset in HIV^- and HIV^+ PBMCs were examined by flow cytometry. HIV^+ patients were divided into five groups based on nadir CD4 counts as indicated in the figure. One asterisk (*) shows a *p*-value less than 0.05, and *p*-values less than 0.01 are marked with two asterisks (**). Student's *t*-test was performed to determine the p-values in comparison with the HIV^- control group.

with ART, we longitudinally examined changes in the $CD4^+$ T-cell subsets in 18 chronic patients (Supplementary Table 2). They were selected from the 34 patients based on the availability of samples. We divided them into three groups based on their nadir CD4 counts: <100 cells/μl (nadir <100 group, $n = 8$), 100–250 cells/μl (nadir 100–250 group, $n = 7$), and >250 cells/μl (nadir >250 group, $n = 3$). In each group, we studied the distributions of CD4 T-cell subsets at four time points: more than six months prior to the nadir time point (before nadir), six months before and after the nadir time point (around nadir), six months to three years after the nadir time point (<3yrs after nadir), and three years or longer after the nadir point (= or >3 yrs after nadir). A drastic reduction of the naïve subset occurred in the nadir <100 group at the nadir time point (Fig. 3A, green bars in the left panel). During this period, only 13.1% of the peripheral $CD4^+$ T-cell pool were naïve compared to 36.7% and 47.2% in the nadir 100–250 and >250 groups, respectively. The highly skewed subset profile continued, albeit lessened, until the end of the study in the nadir <100 group (3–11 years after the nadir point, Fig. 3A). Even at this time point, the decreased naïve subset did not show a sign of recovery, reaching only to 25.2% of the peripheral $CD4^+$ T-cell pool. The proportions of all four subsets were still significantly different from those in HIV^- individuals, even though ART successfully increased CD4 counts in the nadir <100 group (Fig. 3A).

Only mild deviations were observed in the patients who maintained at least 100 $CD4^+$ T cells/μl. The nadir 100–250 group had 6.8% of $CD4^+$ T cells ($p = 0.043$) in the T_{EM} subset, and >250 group had 6.5% ($p = 0.049$) after three years post CD4 nadir points, both of which were statistically different from the frequency of the T_{EM} subset observed in uninfected individuals (Fig. 3A, yellow bars). However, the subset-distribution patterns in the both groups stayed similar to that in the HIV^- control subjects throughout the duration of the experiment (Fig. 3A). These observations suggested a substantial effect of CD4 nadir count on the balanced distribution of CD4 functional subsets and possibly CD4 immune function.

The absolute number of cells in each subset also showed a similar trend. For the first three years of recovery after the CD4 nadir (<3 yr after nadir), the number of naïve cells was approximately 5.5 times less in the nadir <100 group (mean 36 cells/μl) than in the other two groups (mean 195 and 210 cells/μl, respectively), even though their CD4 counts were elevated by ART to a level equivalent to those in the other groups (Fig. 3B). Drastic difference was also observed in effector cells during the first three years post CD4 nadir. The absolute number was 2.8 and 6.0 times more in the nadir <100 group than in the 100–250 and >250 groups, respectively (Fig. 3B), being partially responsible for the imbalanced subset distribution. Concomitantly, a steady increase was observed in the subsets defined as $CD45RA^-$ $CCR7^+$ $CD27^-$ $CD28^+$ and $CD45RA^-$ $CCR7^-$ $CD27^-$ $CD28^+$ in the nadir <100 group (data not shown), but the function of these subsets remains to be determined. The number of total $CD4^+$ T cells did not fully recover in the nadir <100 and 100–250 groups even though they were on ART for years and aviremic. Therefore, it was not possible to make a fair comparison between patients with nadir CD4 counts less than and above

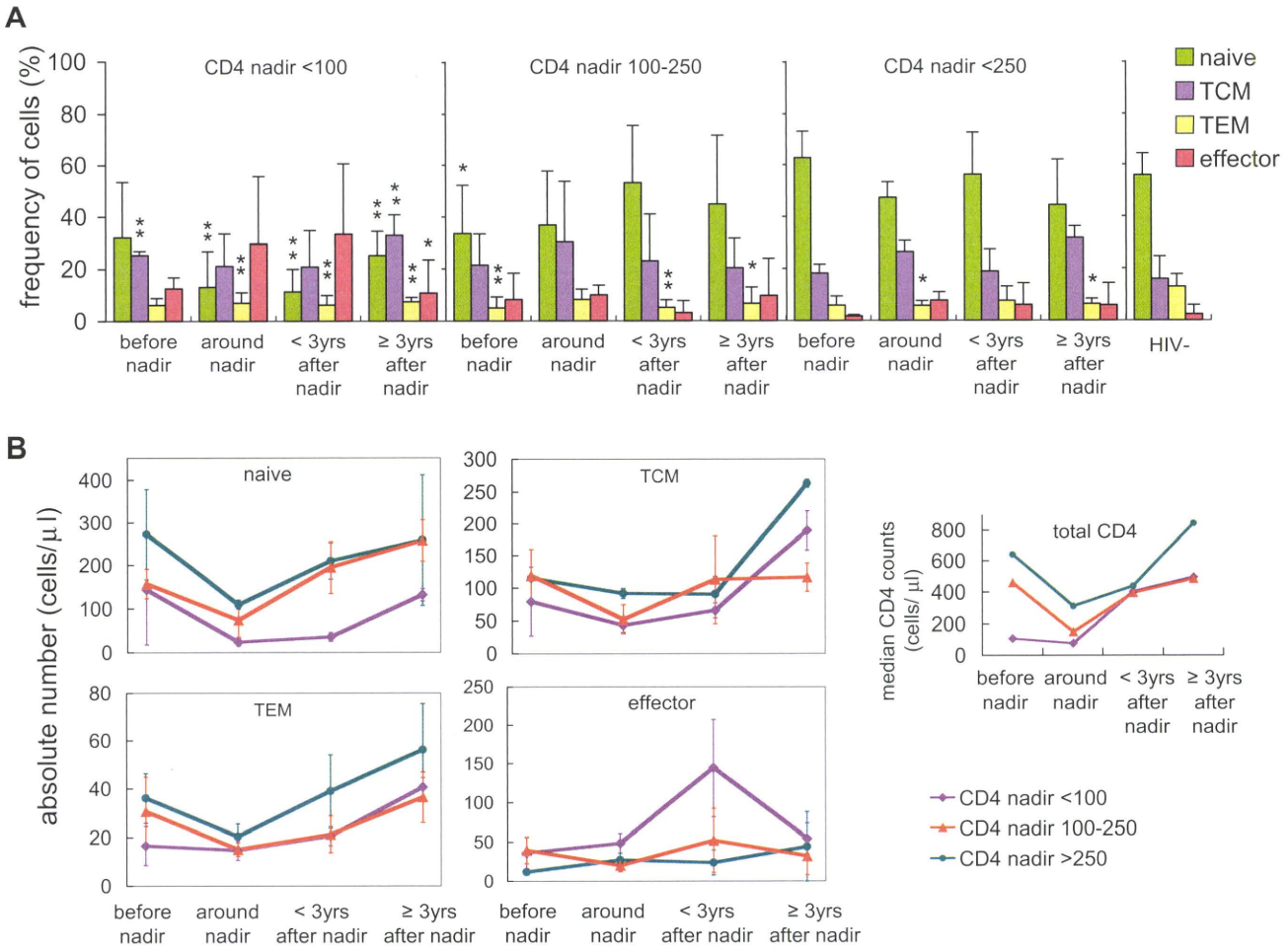

Fig. 3. Longitudinal analysis of the distribution of $CD4^+$ T-cell subsets in HIV^+ patients. (A) Frequency of each functional subset in the peripheral $CD4^+$ T-cell pool was phenotypically defined as described in the Fig. 1. Eighteen patients were divided into three groups: those who had nadir CD4 counts less than 100 cells/μl (CD4 nadir <100), between 100 and 250 cells/μl (CD4 nadir 100–250), and at least 250 cells/μl (CD4 nadir >250). The subset distributions in each group of patients were examined at four different time points, (1) more than 6 months before the CD4 nadir point (before nadir), (2) within 6 months of the nadir point (around nadir), (3) 6 months to 3 years after the nadir point (<3 yrs after nadir), and (4) more than 3 years since the nadir point (3 or more yrs after nadir). The upper insets (line graphs) indicate changes in the mean CD4 counts. Naïve cells are defined as $CD45RA^+$ $CCR7^+$ $CD27^+$ $CD28^+$ cells (shown in green) and T_{CM} as $CD45RA^-$ $CCR7^+$ $CD27^+$ $CD28^+$ cells (shown in purple). $CD45RA^-$ $CCR7^-$ $CD27^+$ $CD28^+$ and $CD45RA^-$ $CCR7^-$ $CD27^-$ $CD28^-$ cells represent T_{EM} (yellow bars) and effector (pink bars), respectively. *p*-Values were determined in comparison with the HIV^- group by Student's *t*-test, and values less than 0.05 and 0.01 are marked with one and two asterisks, respectively. (B) The mean absolute numbers of peripheral $CD4^+$ T cells in each functional subset were determined based on the CD4 count and the frequency of cells in each subset at the indicated time period. The pink line indicates the mean naïve $CD4^+$ T-cell number in patients with nadir CD4 counts <100 cells/μl. The orange and the blue lines show patients whose CD4 nadir counts were 100–250 and at least 250 cells/μl, respectively.

250. Together, our results suggest that nadir CD4 counts severely affected the proper maintenance of the functional CD4 T-cell subsets.

4. Discussion

HIV-1 infection induces massive depletion of $CD4^+$ memory T cells and the accumulation of effector cells in lymph nodes [42,43], which could cause the disruption of normal T-cell homeostasis and functions. A number of reports indicated that HAART did not effectively restore antigen-specific proliferation and immune responsiveness of $CD4^+$ T cells in chronic patients unless it was initiated before their $CD4^+$ counts dropped severely [44–47]. To gain a mechanistic insight into virally induced, irreversible $CD4^+$ T-cell dysfunction, we examined the homeostatic balance of functional $CD4^+$ T-cell subsets in chronically infected patients. The phenotypic analysis indicated clear difference between patients with nadir CD4 counts less than 100 cells/μl and those who maintained at least 100 cells/μl CD4 counts (Figs. 2 and 3). The patients with the lower nadir CD4 counts had severely skewed distributions of functional subsets even though ART restored their CD4 counts. The difference was substantial, particularly in the naïve and effector subsets. When compared to HIV^- individuals, only the nadir <100 group showed statistically significant deviations in those two subsets, and the

skewed distribution was more exacerbated in patients with CD4 nadir counts <50 cells/μl (Fig 2B). The abnormality was also detected in the absolute numbers of T_{EM} cells in the patients with lower nadir CD4 counts. The recovery of T_{EM} cells in these patients was considerably slower than those who maintained at least 250 $CD4^+$ T cells/μl (Fig. 3B). Low numbers of naïve $CD4^+$ T cells in these patients may have hindered T-cell maturation and differentiation into T_{EM} cells. Alternatively, T_{EM} cells may have been depleted from the peripheral $CD4^+$ T-cell pool by preferential infection as indicated by a recent study [48].

Our data suggested that HIV-1 infection caused prolonged homeostatic imbalance of functional subsets in the peripheral $CD4^+$ T cells, and nadir CD4 counts were negatively correlated with the magnitude of the imbalance. The abnormal subset distribution in the nadir <100 group was slightly alleviated with 3–11 years of ART; the naïve subset increased as the effector subset dropped to the initial level (Fig. 3). However, the recovery of the naïve subset was mild and still did not reach to the level attained by patients with nadir CD4 counts above 100 cells/μl. Moreover, the proportion of T_{CM} remained excessively high, resulting in twice the frequency of the uninfected naïve subset. A progressive increase also occurred in the subsets defined as $CD45RA^-$ $CCR7^+$ $CD27^-$ $CD28^+$ and $CD45RA^-$ $CCR7^-$ $CD27^-$ $CD28^+$ cells. The former subset is not well defined because of extremely low frequency in the uninfected $CD4^+$ T-cell pool [3,5,7,10–13]. The presence of CCR7 and the loss of CD45RA and CD27 markers on these cells suggest that they probably have a memory phenotype which is more differentiated than T_{CM} but not as mature as T_{EM}. The latter subset predominantly consists of a heterogeneous population of T_h1 and T_h2 T_{EM}/effector cells [3,5,7,10–13]. It is tempting to speculate that the chronic immune activation in HIV^+ patients led to the loss of naïve cells and increase in subsets with memory/effector functions as short-lived effector cells decreased.

Our study indicated a slower recovery of total CD4 counts in patients with nadir CD4 counts less than 250 cells/μl even after years of ART, showing retarded rates of recovery particularly in the numbers of naïve and memory cells. Difference in the recovery rates was evident in the absolute numbers of naïve cells in the nadir <100 group, T_{CM} cells in the 100–250 group, and T_{EM} cells in the both groups (Fig. 3B). However, only the <100 group showed a drastically distorted distribution of $CD4^+$ T-cell subsets while the nadir 100–250 group maintained a distribution similar to that observed in the >250 group and uninfected individuals. These observations suggested that ART failed to recover the proper frequency of each functional compartment once patients' CD4 fell extremely low, even though it successfully restored the quantitative defect in the peripheral $CD4^+$ T-cell pool. The irreversible subset imbalance was more exacerbated when CD4 nadir reached below 50 cells/μl, supporting a correlation between prognosis and the CD4 counts at which ART was initiated [39–41]. The cause of impaired maintenance of proper $CD4^+$ T-cell compartments in low nadir CD4 patients is yet to be defined. The virus may affect the normal development and maturation of $CD4^+$ T cells directly or indirectly, or the chronic immune activation may prevent the proper reconstitution of the functional subsets in HIV^+ patients.

Acknowledgements

We thank Drs. Takamasa Ueno for helpful comments, and Madoka Koyanagi and Hayato Murakoshi for sample preparation. We are also grateful to Sachiko Sakai for secretarial assistance. This research was supported by grant-in-aid for scientific research from the Ministry of Health (No. 20390134) and the Ministry of Education, Science, Sports and Culture, Japan (No. 18390141) to MT.

Appendix A. Supplementary information

Supplementary data associated with this article can be found in the online version, at doi:10.1016/j.micinf.2010.01.013.

References

[1] D. Masopust, V. Vezys, A.L. Marzo, L. Lefrancois, Preferential localization of effector memory cells in nonlymphoid tissue. Science 291 (2001) 2413.
[2] C.Y. Wu, J.R. Kirman, M.J. Rotte, D.F. Davey, S.P. Perfetto, Distinct lineages of TH1 cells have differential capacities for memory cell generation in vivo. Nat. Immunol. 3 (2002) 852.
[3] F. Sallusto, D. Lenig, R. Forster, M. Lipp, A. Lanzavecchia, Two subsets of memory T lymphocytes with distinct homing potentials and effector functions. Nature 401 (1999) 708–712.
[4] F. Sallusto, J. Geginat, A. Lanzavecchia, Central memory and effector memory T cell subsets: function, generation, and maintenance. Annu. Rev. Immunol. 22 (2004) 745–763.
[5] E. Amyes, A.J. McMichael, M.F.C. Callan, Human CD4+ T cells are predominantly distributed among six phenotypically and functionally distinct subsets. J. Immunol. 175 (2005) 5765–5773.
[6] A. Harari, F. Vallelian, G. Pantaleo, Phenotypic heterogeneity of antigen-specific CD4 T cells under different conditions of antigen persistence and antigen load. Eur. J. Immunol. 34 (2004) 3525–3533.
[7] R. Okada, T. Kondo, F. Matsuki, H. Takata, M. Takiguchi, Phenotypic classification of human CD4+ T cell subsets and their differentiation. Int. Immunol. 20 (2008) 1189–1199.
[8] V. Appay, R.A. van Lier, F. Sallusto, M. Roederer, Phenotype and function of human T lymphocyte subsets: consensus and issues. Cytometry A 73 (2008) 975–983.
[9] S.C. De Rosa, L.A. Herzenberg, L.A. Herzenberg, M. Roederer, 11-color, 13-parameter flow cytometry: identification of human naive T cells by phenotype, function, and T-cell receptor diversity. Nat. Med. 7 (2001) 245–248.
[10] V. Appay, A. Bosio, S. Lokan, Y. Wiencek, C. Biervert, D. Kusters, E. Devevre, D. Speiser, P. Romero, N. Rufer, S. Leyvraz, Sensitive gene expression profiling of human T cell subsets reveals parallel post-thymic differentiation for CD4+ and CD8+ lineages. J. Immunol. 179 (2007) 7406–7414.
[11] K. Sugita, T. Hirose, D.M. Rothstein, C. Donahue, S.F. Schlossman, C. Morimoto, CD27, a member of the nerve growth factor receptor family, is preferentially expressed on CD45RA+ CD4 T cell clones and involved in distinct immunoregulatory functions. J. Immunol. 149 (1992) 3208–3216.
[12] R.D. Fritsch, X. Shen, G.P. Sims, K.S. Hathcock, R.J. Hodes, P.E. Lipsky, Stepwise differentiation of CD4 memory t cells defined by expression of CCR7 and CD27. J. Immunol. 175 (2005) 6489–6497.

[13] C.S. Ma, P.D. Hodgkin, S.G. Tangye, Automatic generation of lymphocyte heterogeneity: division-dependent changes in the expression of CD27, CCR7 and CD45 by activated human naive CD4+ T cells are independently regulated. Immunol. Cell Biol. 82 (2004) 67–74.
[14] H.C. Lane, J.M. Depper, W.C. Greene, G. Whalen, T.A. Waldmann, A.S. Fauci, Qualitative analysis of immune function in patients with the acquired immunodeficiency syndrome. Evidence for a selective defect in soluble antigen recognition. N. Engl. J. Med. 313 (1985) 79–84.
[15] H.W. Murray, B.Y. Rubin, H. Masur, R.B. Roberts, Impaired production of lymphokines and immune (gamma) interferon in the acquired immunodeficiency syndrome. N. Engl. J. Med. 310 (1984) 883–889.
[16] J.S. Epstein, W.R. Frederick, A.H. Rook, L. Jackson, J.F. Manischewitz, R.E. Mayner, H. Masur, J.C. Enterline, J.Y. Djeu, G.V.J. Quinnan, Selective defects in cytomegalovirus- and mitogen-induced lymphocyte proliferation and interferon release in patients with acquired immunodeficiency syndrome. J. Infect. Dis. 152 (1985) 727–733.
[17] M. Roos, F. Miedema, M. Koot, M. Tersmette, W. Schaasberg, R. Coutinho, P. Schellekens, T cell function in vitro is an independent progression marker for AIDS in human immunodeficiency virus-infected asymptomatic subjects. J. Infect. Dis. 171 (1995) 531–536.
[18] M. Connors, J.A. Kovacs, S. Krevat, J.C. Gea-Banacloche, M.C. Sneller, M. Flanigan, J.A. Metcalf, R.E. Walker, J. Falloon, M. Baseler, R. Stevens, I. Feuerstein, H. Masur, H.C. Lane, HIV infection induces changes in CD4+ T-cell phenotype and depletions within the CD4+ T-cell repertoire that are not immediately restored by antiviral or immune-based therapies. Nat. Med. 3 (1997) 533–540.
[19] S.M. Schnittman, H.C. Lane, J. Greenhouse, J.S. Justement, M. Baseler, A.S. Fauci, Preferential infection of CD4+ memory T cells by human immunodeficiency virus type 1: evidence for a role in the selective T-cell functional defects observed in infected individuals. Proc. Natl. Acad. Sci. U.S.A. 87 (1990) 6058–6062.
[20] C. Chou, V. Gudeman, S. O'Rourke, V. Isacescu, R. Detels, G. Williams, R. Mitsuyasu, J. Giorgi, Phenotypically defined memory CD4+ cells are not selectively decreased in chronic HIV disease. J. Acquir. Immune Defic. Syndr. 7 (1994) 665–675.
[21] D.L. Bowen, H.C. Lane, A.S. Fauci, Immunopathogenesis of the acquired immunodeficiency syndrome. Ann. Intern. Med. 103 (1985) 704–709.
[22] G. Gorochov, A.U. Neumann, A. Kereveur, C. Parizot, T. Li, C. Katlama, M. Karmochkine, G. Raguin, B. Autran, P. Debre, Perturbation of CD4+ and CD8+ T-cell repertoires during progression to AIDS and regulation of the CD4+ repertoire during antiviral therapy. Nat. Med. 4 (1998) 215–221.
[23] G.P. Linette, R.J. Hartzman, J.A. Ledbetter, C.H. June, HIV-1-infected T cells show a selective signaling defect after perturbation of CD3/antigen receptor. Science 241 (1988) 573–576.
[24] M. Clerici, N.I. Stocks, R.A. Zajac, R.N. Boswell, D.R. Lucey, C.S. Via, G.M. Shearer, Detection of three distinct patterns of T helper cell dysfunction in asymptomatic, human immunodeficiency virus-seropositive patients. Independence of CD4+ cell numbers and clinical staging. J. Clin. Invest. 84 (1989) 1892–1899.
[25] F. Miedema, A.J. Petit, F.G. Terpstra, J.K. Schattenkerk, F. de Wolf, B.J. Al, M. Roos, J.M. Lange, S.A. Danner, J. Goudsmit, Immunological abnormalities in human immunodeficiency virus (HIV)-infected asymptomatic homosexual men. HIV affects the immune system before CD4+ T helper cell depletion occurs. J. Clin. Invest. 82 (1988) 1908–1914.
[26] M.J. Fuller, A.J. Zajac, Ablation of CD8 and CD4 T cell responses by high viral loads. J. Immunol. 170 (2003) 477–486.
[27] S.A. Ghanekar, S.A. Stranford, J.C. Ong, J.M. Walker, V.C. Maino, J.A. Levy, Decreased HIV-specific CD4 T cell proliferation in long-term HIV-infected individuals on antiretroviral therapy. AIDS 15 (2001) 1885–1887.
[28] A. Harari, S. Petitpierre, F. Vallelian, G. Pantaleo, Skewed representation of functionally distinct populations of virus-specific CD4 T cells in HIV-1-infected subjects with progressive disease: changes after antiretroviral therapy. Blood 103 (2004) 966–972.
[29] C. Iyasere, J.C. Tilton, A.J. Johnson, S. Younes, B. Yassine-Diab, R.-P. Sekaly, W.W. Kwok, S.A. Migueles, A.C. Laborico, W.L. Shupert, C.W. Hallahan, R.T. Davey Jr., M. Dybul, S. Vogel, J. Metcalf, M. Connors, Diminished proliferation of human immunodeficiency virus-specific CD4+ T cells is associated with diminished interleukin-2 (IL-2) production and is recovered by exogenous IL-2. J. Virol. 77 (2003) 10900–10909.
[30] A.C. McNeil, W.L. Shupert, C.A. Iyasere, C.W. Hallahan, J. Mican, R.T. Davey, M. Connors, High-level HIV-1 viremia suppresses viral antigen-specific CD4+ T cell proliferation. Proc. Natl. Acad. Sci. U.S.A. 98 (2001) 13878–13883.
[31] A. Oxenius, R.M. Zinkernagel, H. Hengartner, Comparison of activation versus induction of unresponsiveness of virus-specific CD4+ and CD8+ T cells upon acute versus persistent viral infection. Immunity 9 (1998) 449–457.
[32] B.E. Palmer, N. Blyveis, A.P. Fontenot, C.C. Wilson, Functional and phenotypic characterization of CD57+ CD4+ T cells and their association with HIV-1-induced T cell dysfunction. J. Immunol. 175 (2005) 8415–8423.
[33] B.E. Palmer, E. Boritz, N. Blyveis, C.C. Wilson, Discordance between frequency of human immunodeficiency virus type 1 (HIV-1)-specific gamma interferon-producing CD4+ T cells and HIV-1-specific lymphoproliferation in HIV-1-infected subjects with active viral replication. J. Virol. 76 (2002) 5925–5936.
[34] B.E. Palmer, E. Boritz, C.C. Wilson, Effects of sustained HIV-1 plasma viremia on HIV-1 gag-Specific CD4+ T cell maturation and function. J. Immunol. 172 (2004) 3337–3347.
[35] C.J. Pitcher, C. Quittner, D.M. Peterson, M. Connors, R.A. Koup, V.C. Maino, L.J. Picker, HIV-1-specific CD4+ T cells are detectable in most individuals with active HIV-1 infection, but decline with prolonged viral suppression. Nat. Med. 5 (1999) 518–525.
[36] E.S. Rosenberg, J.M. Billingsley, A.M. Caliendo, S.L. Boswell, P.E. Sax, S.A. Kalams, B.D. Walker, Vigorous HIV-1-specific CD4+ T cell responses associated with control of viremia. Science 278 (1997) 1447–1450.
[37] J.D.K. Wilson, N. Imami, A. Watkins, J. Gill, P. Hay, B. Gazzard, M. Westby, F.M. Gotch, Loss of CD4+ T cell proliferative ability but not loss of human immunodeficiency virus type 1 specificity equates with progression to disease. J. Infect. Dis. 182 (2000) 792–798.
[38] S.-A. Younes, B. Yassine-Diab, A.R. Dumont, M.-R. Boulassel, Z. Grossman, J.-P. Routy, R.-P. Sekaly, HIV-1 viremia prevents the establishment of interleukin 2-producing HIV-specific memory CD4+ T cells endowed with proliferative capacity. J. Exp. Med. 198 (2003) 1909–1922.
[39] When to start consortium, timing of initiation of antiretroviral therapy in AIDS-free HIV-1-infected patients: a collaborative analysis of 18 HIV cohort studies. Lancet 373 (2009) 1352–1363.
[40] Strategies for Management of Antiretroviral Therapy (SMART) Study Group, Major clinical outcomes in antiretroviral therapy (ART)-naive participants and in those not receiving ART at baseline in the SMART study. J. Infect. Dis. 197 (2008) 1133–1144.
[41] M.M. Kitahata, S.J. Gange, A.G. Abraham, B. Merriman, M.S. Saag, A. C. Justice, R.S. Hogg, S.G. Deeks, J.J. Eron, J.T. Brooks, S.B. Rourke, M.J. Gill, R.J. Bosch, J.N. Martin, M.B. Klein, L.P. Jacobson, B. Rodriguez, T.R. Sterling, G.D. Kirk, S. Napravnik, A.R. Rachlis, L.M. Calzavara, M.A. Horberg, M.J. Silverberg, K.A. Gebo, J.J. Goedert, C. A. Benson, A.C. Collier, S.E. Van Rompaey, H.M. Crane, R.G. McKaig, B. Lau, A.M. Freeman, R.D. Moore, the NA-ACCORD Investigators, Effect of early versus deferred antiretroviral therapy for HIV on survival. N. Engl. J. Med. 360 (2009) 1815–1826.
[42] J.M. Brenchley, T.W. Schacker, L.E. Ruff, D.A. Price, J.H. Taylor, G.J. Beilman, P.L. Nguyen, A. Khoruts, M. Larson, A.T. Haase, D.C. Douek, CD4+ T cell depletion during all stages of HIV disease occurs predominantly in the gastrointestinal tract. J. Exp. Med. 200 (2004) 749–759.
[43] Q. Li, L. Duan, J.D. Estes, Z.-M. Ma, T. Rourke, Y. Wang, R. Cavan, J. Carlis, C.J. Miller, A.T. Haase, Peak SIV replication in resting memory CD4+ T cells depletes gut lamina propria CD4+ T cells. Nature 434 (2005) 1148–1152.
[44] C.G. Lange, M.M. Lederman, K. Medvik, R. Asaad, M. Wild, R. Kalayjian, H. Valdez, Nadir CD4+ T-cell count and numbers of CD28+

CD4+ T-cells predict functional responses to immunizations in chronic HIV-1 infection. AIDS 17 (2003) 2015–2023.

[45] C.G. Lange, H. Valdez, K. Medvik, R. Asaad, M.M. Lederman, CD4+ T-lymphocyte nadir and the effect of highly active antiretroviral therapy on phenotypic and functional immune restoration in HIV-1 infection. Clin. Immunol. 102 (2002) 154–161.

[46] M. Elrefaei, M.D. McElroy, C.P. Preas, R. Hoh, S. Deeks, J. Martin, H. Cao, Central Memory $CD4^+$ T cell responses in chronic HIV infection are not restored by antiretroviral therapy. J. Immunol. 173 (2004) 2184–2189.

[47] M. Guadalupe, E. Reay, S. Sankaran, T. Prindiville, J. Flamm, A. McNeil, S. Dandekar, Severe CD4+ T-cell depletion in gut lymphoid tissue during primary human immunodeficiency virus type 1 infection and substantial delay in restoration following highly active antiretroviral therapy. J. Virol. 77 (2003) 11708–11717.

[48] N. Chomont, M. El-Far, P. Ancuta, L. Trautmann, F.A. Procopio, B. Yassine-Diab, G. Boucher, M.-R. Boulassel, G. Ghattas, J.M. Brenchley, T.W. Schacker, B.J. Hill, D.C. Douek, J.-P. Routy, E.K. Haddad, R.-P. Sekaly, HIV reservoir size and persistence are driven by T cell survival and homeostatic proliferation. Nat. Med. 15 (2009) 893–900.

ANTIMICROBIAL AGENTS AND CHEMOTHERAPY, Apr. 2010, p. 1596–1602 Vol. 54, No. 4
0066-4804/10/$12.00 doi:10.1128/AAC.01480-09

Combination of V106I and V179D Polymorphic Mutations in Human Immunodeficiency Virus Type 1 Reverse Transcriptase Confers Resistance to Efavirenz and Nevirapine but Not Etravirine▽†

Hiroyuki Gatanaga,[1,2]* Hirotaka Ode,[4] Atsuko Hachiya,[1,3] Tsunefusa Hayashida,[1,2] Hironori Sato,[4] and Shinichi Oka[1,2]

AIDS Clinical Center, International Medical Center of Japan, Tokyo,[1] Divisions of Infectious Disease[2] and Viral Immunology,[3] Center for AIDS Research, Kumamoto University, Kumamoto, and Laboratory of Viral Genomics, Pathogen Genomics Center, National Institute of Infectious Diseases, Tokyo,[4] Japan

Received 19 October 2009/Returned for modification 16 December 2009/Accepted 22 January 2010

Etravirine (ETV) is a second-generation nonnucleoside reverse transcriptase (RT) inhibitor (NNRTI) introduced recently for salvage antiretroviral treatment after the emergence of NNRTI-resistant human immunodeficiency virus type 1 (HIV-1). Following its introduction, two naturally occurring mutations in HIV-1 RT, V106I and V179D, were listed as ETV resistance-associated mutations. However, the effect of these mutations on the development of NNRTI resistance has not been analyzed yet. To select highly NNRTI-resistant HIV-1 *in vitro*, monoclonal HIV-1 strains harboring V106I and V179D (HIV-1_{V106I} and HIV-1_{V179D}) were propagated in the presence of increasing concentrations of efavirenz (EFV). Interestingly, V179D emerged in one of three selection experiments from HIV-1_{V106I} and V106I emerged in two of three experiments from HIV-1_{V179D}. Analysis of recombinant HIV-1 clones showed that the combination of V106I and V179D conferred significant resistance to EFV and nevirapine (NVP) but not to ETV. Structural analysis indicated that ETV can overcome the repulsive interactions caused by the combination of V106I and V179D through fine-tuning of its binding module to RT facilitated by its plastic structure, whereas EFV and NVP cannot because of their rigid structures. Analysis of clinical isolates showed comparable drug susceptibilities, and the same combination of mutations was found in some database patients who experienced virologic NNRTI-based treatment failure. The combination of V106I and V179D is a newly identified NNRTI resistance pattern of mutations. The combination of polymorphic and minor resistance-associated mutations should be interpreted carefully.

Human immunodeficiency virus type 1 (HIV-1) sequences differ among infected individuals, and there are a number of naturally occurring amino acid changes commonly found in treatment-naïve patients (3, 23, 28). These polymorphic changes can occur even in genes that encode drug target proteins, and in fact, some drug resistance-associated mutations in protease genes are often present in treatment-naïve individuals, especially in non-subtype B clade-infected individuals (13, 15, 22). Minor resistance mutations, which are considered to compensate for the impaired replication fitness of viruses containing major resistance mutations, do not have a substantial effect on the viral phenotype by themselves (14, 27). In the reverse transcriptase (RT) coding region, drug resistance-associated mutations were detected at a low frequency in treatment-naïve individuals regardless of the HIV-1 clade. However, etravirine (ETV), a second-generation nonnucleoside RT inhibitor (NNRTI), has been available in the clinical setting and the following have been listed as ETV resistance-associated mutations in RT: V90I, A98G, L100I, K101E/H/P, V106I, E138A, V179D/F/T, Y181C/I/V, G190S/A, and M230L (14). V106I and V179D are often found in treatment-naïve individuals but are considered to have no substantial impact on NNRTI-containing treatment by themselves. ETV exhibits activity against many viruses that are resistant to first-line NNRTIs, including efavirenz (EFV) and nevirapine (NVP), and shows clinical efficacy in salvage treatment after NNRTI treatment failure (18, 21). However, it is possible that EFV- and NVP-resistant viruses derived from HIV-1 harboring V106I or V179D could compromise the efficacy of ETV. To determine the impact of these polymorphic mutations on the mutation patterns of NNRTI resistance, EFV-resistant HIV-1 strains were selected *in vitro* from monoclonal viruses harboring V106I and V179D, respectively. The virologic effects of selected specific mutation patterns were analyzed by constructing recombinant HIV-1 clones, and their clinical relevance was confirmed by analysis of isolates from infected individuals.

MATERIALS AND METHODS

HIV-1 sequences and clinical isolates from treatment-naïve individuals. HIV-1 RT sequences were analyzed in 364 antiretroviral treatment-naïve infected individuals who visited the outpatient clinic of the AIDS Clinical Center, International Medical Center of Japan, in 2007 and 2008 and gave written informed consent to this study. Viral RNA was extracted from stocked plasma samples, and the HIV-1 RT coding region was amplified by RT-PCR and nested PCR using previously published primer pairs (7, 10, 11). Direct sequencing was performed using dye terminators, and the HIV-1 subtypes of the sequences obtained were determined by the neighbor-joining method. Clinical HIV-1 isolates were obtained using MAGIC-5 cells (CCR5- and CD4-expressing HeLa-LTR-β-D-gal cells) from fresh plasma samples collected from seven of the above-mentioned treatment-naïve patients and stored at −80°C until use (9).

* Corresponding author. Mailing address: AIDS Clinical Center, International Medical Center of Japan, 1-21-1 Toyama, Shinjuku-ku, Tokyo 162-8655, Japan. Phone: 81-3-3202-7181. Fax: 81-3-5273-6483. E-mail: higatana@imcj.acc.go.jp.

† Supplemental material for this article may be found at http://aac.asm.org/.

▽ Published ahead of print on 1 February 2010.

TABLE 1. Frequencies of amino acids at positions associated with NNRTI resistance mutations in HIV-1 RT in treatment-naïve patients

Position	Amino acid, frequency [*n* (%)/364][a]						
90	V, 361 (99.2)	I, 3 (0.8)					
98	A, 344 (94.5)	S, 20 (5.5)					
101	K, 352 (96.7)	Q, 8 (2.2)	R, 3 (0.8)	E, 1 (0.3)			
103	K, 353 (97.0)	R, 7 (1.9)	N, 2 (0.5)	Q, 2 (0.5)			
106	V, 355 (97.5)	I, 9[b] (2.5)					
108	V, 362 (99.5)	I, 2 (0.5)					
138	E, 361 (99.2)	K, 1 (0.3)	A, 1 (0.3)	G, 1 (0.3)			
179	V, 312 (85.7)	D, 21[c] (5.8)	I, 21 (5.8)	E, 4 (1.1)	A, 4 (1.1)	T, 1 (0.3)	N, 1 (0.3)

[a] Only wild-type amino acids (L, Y, Y, G, P, and M, respectively) were identified at the 100th, 181st, 188th, 190th, 225th, and 230th positions of HIV-1 RT.
[b] Including two cases with V90/A98/K101Q/K103/V106I/V108/E138/V179, two cases with V90/A98/K101/K103/V106I/V108/E138/V179I, one case with V90/A98/K101/K103/V106I/V108/E138/V179D, and four cases with V90/A98/K101/K103/V106I/V108/E138/V179.
[c] Including 2 cases with V90/A98S/K101/K103/V106/V108/E138/V179D, 1 case with V90/A98/K101E/K103R/V106/V108/E138/V179D, 1 case with V90/A98/K101/K103R/V106/V108/E138/V179D, 1 case with V90/A98/K101/K103/V106I/V108/E138/V179D, and 16 cases with V90/A98/K101/K103/V106/V108/E138/V179D.

Generation of recombinant HIV-1 strains. The desired mutations were introduced into the XmaI-NheI region of pTZNX, which encodes Gly-15 to Ala-267 of HIV-1 RT (strain BH 10), by the oligonucleotide-based mutagenesis method (10, 16). The XmaI-NheI fragment was inserted into pNL_{H219Q}, which was modified from pNL101 and encoded the full genome of HIV-1 strain BH 10. pNL_{H219Q} harbors the H219Q mutation in the HIV-1 Gag region, which facilitated HIV-1 replication in MT-2 and H9 cells (6, 8). HIV-1 derived from pNL_{H219Q} was used as the wild type. Determination of the nucleotide sequences of the plasmids confirmed that each clone had the desired mutations but was devoid of unintended mutations. Each molecular clone was transfected into COS-7 cells with the GenePORTER Transfection Reagent (Gene Therapy Systems, San Diego, CA), and the virions obtained were harvested 48 h after transfection and stored at −80°C until use.

Selection of EFV-resistant HIV-1. The infectious HIV-1 clones harboring the V106I (HIV-1_{V106I}) and V179D (HIV-1_{V179D}) mutations in their RTs were propagated in MT-2 cells in the presence of increasing concentrations of EFV (7, 8, 31). Briefly, MT-2 cells (1×10^5) were exposed to 500 blue-cell-forming units (BFU) in MAGIC-5 cells containing HIV-1_{V106I} and HIV-1_{V179D} and cultured in the presence of EFV at an initial concentration of 3 nM. Viral replication was monitored by observation of the cytopathic effect in MT-2 cells. The culture supernatant was harvested on day 7 of culture and used to infect fresh MT-2 cells for the next round of culture. When the virus began to propagate in the presence of the drug, the drug concentration was increased by 0.5-log-fold. This selection was carried out for a total of 14 passages. The proviral HIV-1 RT coding region in infected MT-2 cells was amplified and sequenced at several passages.

Drug susceptibility assay. EFV, NVP, and ETV were generously provided by Merck Co., Inc. (Rahway, NJ), Boehringer Ingelheim Pharmaceutics Inc. (Ridgefield, CT), and Tibotec Pharmaceuticals (Little Island, Co., Cork, Ireland), respectively. Recombinant and isolated HIV-1 susceptibility to EFV, NVP, and ETV was determined in triplicate using MAGIC-5 cells (10, 12, 16). Briefly, MAGIC-5 cells were infected with an adjusted virus stock (300 BFU) in various concentrations of NNRTIs, cultured for 48 h, fixed, and stained with 5-bromo-4-chloro-3-indolyl-β-D-galactopyranoside (Takara Shuzo, Ohtsu, Japan). The blue-stained cells were counted under a light microscope. The drug concentrations that inhibited 50% of the stained cells of a drug-free control (EC_{50}s) were determined by referring to the dose-response curve. The drug susceptibility assay was performed in triplicate and repeated three times. Fold resistance was calculated by comparing the viral EC_{50} with that of monoclonal wild-type HIV-1 (HIV-1_{WT}). Drug resistance was judged significant when it was higher than threefold.

Viral replication kinetics assay. MT-2 cells (1×10^5) were exposed to each infectious virus preparation (500 BFU) for 2 h, washed twice with phosphate-buffered saline (PBS), and cultured in the presence or absence of 10 nM EFV, 100 nM NVP, or 10 nM ETV. The culture supernatants were harvested every other day, and p24 Gag amounts were determined with a chemiluminescence enzyme immunoassay kit (Fuji-Rebio, Tokyo, Japan). Replication assays were performed in triplicate and repeated three times using independently generated virus preparations (7).

Competitive HIV-1 replication assay. Freshly prepared H9 cells (3×10^5) were exposed to mixtures of paired virus preparations (300 BFU each) to be examined for their replication ability for 2 h, washed twice with phosphate-buffered saline (PBS), and cultured in the absence or presence of 10 nM EFV or 100 nM NVP as described previously (7, 17). On day 1, one-third of the infected H9 cells were harvested and washed twice with PBS, and proviral DNAs were sequenced (0 week). Every 7 days, the supernatant of the virus culture was transferred to new uninfected H9 cells; the cells harvested at the end of each passage were subjected to direct DNA sequencing of the HIV-1 RT coding region, and the change in the viral population was determined by the relative peak height on the sequencing electrogram. The persistence of the original amino acid substitution was confirmed at the end of the assay.

Structure modeling. We constructed 18 structural models of the HIV-1 RT and NNRTI complex by computational analysis. First, we constructed the initial models of wild-type RT with one of three NNRTIs by homology modeling using Molecular Operating Environment 2007.09.02 (Chemical Computing Group, Montreal, Quebec, Canada). The crystal structures of RT with NNRTIs (Protein Data Bank codes 1IKW [20], 1VRT [26], and 1SV5 [4]) were used as template structures. The homology modeling enabled the building of missing atoms in template structures. The ff94 force field and distance-dependent electrostatic energy function were applied in the modeling. Next, we refined the initial models by energy minimization using the sander module of the AMBER9 software package in two steps. In the first step, energies for the NNRTIs in the complex models were minimized in the gas phase by the conjugated gradient method. When the energy was not converged until 10,000 steps, this step was ignored. In the second step, energies of whole structures were converged up to 0.5 kcal/mol/Å by 50 steps of the steepest-descent method and the subsequent conjugated gradient method under implicit water solvent conditions. In each minimization, the AMBER ff03 (5, 19), the general AMBER force field (30), and the generalized Born implicit solvent surface area method (IGB = 2) (24) were applied for potential energy calculations. The cutoff for long-distance interaction energy was set at 15.0 Å. The charge and type of every atom in NNRTIs were automatically assigned using the AMBER9 Antechamber module. We also constructed five mutant RTs with the NNRTIs by considering every possible conformer of the respective mutant models. The possible conformers were generated from the wild-type homology models using PyMOL ver. 0.99rc6 (http://www.pymol.org). V106A, V106I, and V179D mutants had one, three to five, and five possible conformers, respectively. The structural model of each conformer was refined by a method similar to that used in the wild-type models. Among the refined conformers, we selected the conformer with the lowest energy as each mutant model.

RESULTS

Frequencies of NNRTI resistance mutations in treatment-naïve individuals. To determine the frequency of NNRTI resistance-associated mutations, the HIV-1 RT coding region was analyzed and the viral subtype was determined in 364 treatment-naïve infected individuals. The most frequent subtype was clade B (*n* = 334; 91.8%), followed by clade AE (*n* = 20; 5.5%). Clades C and G were also found and at similar low frequencies (*n* = 5; 1.4%). Variable amino acid substitutions were identified at the positions of NNRTI resistance-associated mutations, including the 90th, 98th, 101st, 103rd, 106th, 108th, 138th, and 179th, though only the wild-type amino acids were observed at the 100th, 181st, 188th, 190th, 225th, and 230th positions of HIV-1 RT (Table 1). K103N and V108I are

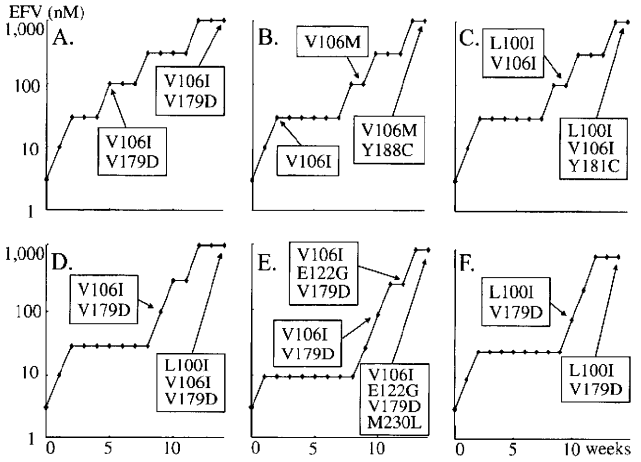

FIG. 1. Selected amino acid substitutions under selective pressure from EFV. HIV-1_{V106I} (A to C) and HIV-1_{V179D} (D to F) were propagated in MT-2 cells in the presence of increasing concentrations of EFV. The selected amino acid substitutions were analyzed at several passages by sequencing the proviral HIV-1 RT coding region in MT-2 cells. Amino acid substitutions compared with wild-type strain BH 10 are shown.

listed as EFV and NVP resistance-associated mutations and V90I, K101E, V106I, E138A, V179D, and V179T are listed as ETV resistance-associated mutations in the Drug Resistance Mutation List of the International AIDS Society (IAS)-USA (14). Of these NNRTI resistance-associated mutations, V106I (2.5%) and V179D (5.8%) were frequently observed in treatment-naïve patients, while the other six mutations were less common (0.3 to 0.8%). These data indicate that V106I and V179D occur naturally in treatment-naïve individuals at significant frequencies and are clinically important as polymorphic mutations. Accordingly, we focused on these two polymorphic mutations and analyzed their effects on the development of NNRTI resistance. There was no overt linkage among the amino acids at the positions of NNRTI resistance-associated mutations, though one patient harbored both V106I and V179D without any other resistance-associated mutations. There was no correlation between clades and the 106th and 179th amino acids.

Selection of EFV-resistant HIV-1 from HIV-1_{V106I} and HIV-1_{V179D}. To analyze the effects of V106I and V179D on the resistance pattern of mutations, EFV-resistant HIV-1 strains were selected from monoclonal HIV-1 strains harboring V106I (HIV-1_{V106I}) or V179D (HIV-1_{V179D}). These selection experiments were performed independently in triplicate. Interestingly, in one of three selection experiments with HIV-1_{V106I}, V179D emerged when the EFV concentration reached 100 nM, and it was persistently identified until the end of the passages without additional mutations (Fig. 1A). In two other experiments with HIV-1_{V106I}, I106M emerged, followed by Y188C, and L100I emerged, followed by Y181C. These four mutations are already known NNRTI resistance-associated mutations (Fig. 1B and C) (1, 14, 25). In one of three experiments with HIV-1_{V179D}, V106I emerged when the EFV concentration reached 100 nM, and L100I further emerged at the end of the experiments (Fig. 1D). In another experiment, V106I emerged when the EFV concentration was 100 nM, and E122G and M230L followed subsequently (Fig. 1E). In the last experiment, L100I emerged when the EFV concentration reached 100 nM, and it remained until the end of the passages without additional mutations (Fig. 1F). In summary, selected by EFV, V179D emerged in one of three experiments from HIV-1_{V106I} and V106I emerged in two of three experiments from HIV-1_{V179D}, suggesting that the combination of two polymorphic mutations, V106I and V179D, alters viral susceptibility to EFV.

NNRTI susceptibility of recombinant HIV-1 strains. To analyze the effects of V106I, V179D, and their combination on NNRTI susceptibility, a panel of recombinant HIV-1 clones was constructed and their EFV, NVP, and ETV EC_{50}s were determined. As expected, the single mutation V106I or V179D did not confer significant resistance to EFV and NVP (Table 2). HIV-1_{V106A} was generated as a reference, and it showed high-fold resistance to NVP but not to EFV, in agreement with previous studies (10, 14). The addition of V179D to HIV-1_{V106A} (HIV-$1_{V106A/V179D}$) increased its resistance to NVP and conferred significant resistance to EFV. The combination of the two polymorphic mutations, V106I and V179D, which emerged in resistance selection experiments with EFV, conferred significant resistance not only to EFV but also to NVP. In the susceptibility assay with ETV, it exhibited potent anti-HIV-1 activity in all of the HIV-1 strains examined, including the NNRTI-resistant clones described above, indicating that ETV has a different binding formulation with RT molecules than EFV and NVP do.

Replication kinetics of recombinant HIV-1 strains. To analyze the effects of single mutations and their combinations on HIV-1 replication efficiency, we assayed the replication kinetics of recombinant HIV-1 strains in MT-2 cells in the absence or presence of an NNRTI. Each replication assay was performed in triplicate and repeated three times. In the absence of

TABLE 2. NNRTI susceptibility of recombinant HIV-1 strains

HIV-1 strain	Mean EC_{50} (μM) ±SD (fold resistance)[a]		
	EFV	NVP	ETV
Wild type	0.002 ± 0.0007	0.05 ± 0.01	0.0012 ± 0
V106A clone	0.003 ± 0.0009 (1.5)	3.43 ± 0.98 (69)	0.0005 ± 0.0001 (0.40)
V106I clone	0.003 ± 0.0003 (1.5)	0.02 ± 0.0012 (0.40)	0.0015 ± 0.0004 (1.3)
V179D clone	0.004 ± 0.0002 (2.0)	0.13 ± 0.02 (2.6)	0.0019 ± 0.0004 (1.6)
V106A V179D clone	0.013 ± 0.004 (6.5)	4.53 ± 0.72 (91)	0.0014 ± 0.0004 (1.2)
V106I V179D clone	0.029 ± 0.007 (15)	0.37 ± 0.12 (7.0)	0.0024 ± 0.0004 (2.0)

[a] The drug susceptibility assay was performed in triplicate and repeated three times (nine experiments). Data are means of nine experiments.

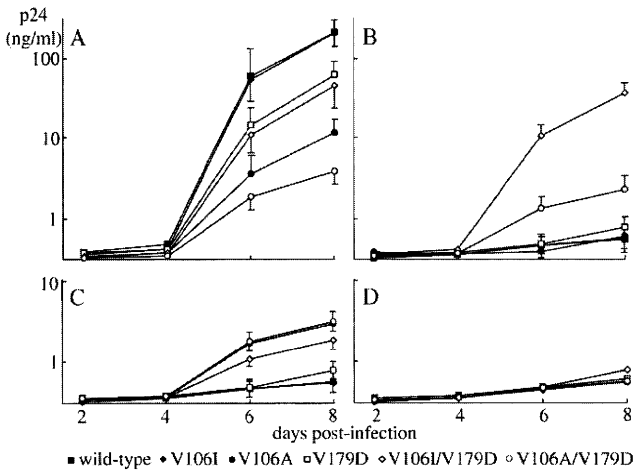

FIG. 2. Replication kinetics of recombinant HIV-1 clones in the absence and presence of NNRTIs. Recombinant HIV-1 clones were propagated in MT-2 cells in the absence (A) and presence of 10 nM EFV (B), 100 nM NVP (C), or 10 nM ETV (D). The concentration of p24 in the culture medium was measured every other day. The assay was performed in triplicate and repeated three times (nine experiments). The data are logarithmic mean p24 concentrations ± standard deviations (days 6 and 8 in panels A to C).

an NNRTI, V106I did not alter HIV-1_{WT} replication while V179D significantly reduced HIV-1_{WT} replication (p24 of HIV-1_{V179D} versus HIV-1_{WT} on day 8; $P < 0.05$) (Fig. 2A). The addition of V106I to HIV-1_{V179D} (HIV-$1_{V106I/179D}$) did not significantly alter its replication kinetics. V106A significantly reduced viral replication (p24 of HIV-1_{V106A} versus HIV-1_{WT} on day 8; $P < 0.01$), and the addition of V179D to it (HIV-$1_{V106A/179D}$) further reduced the virus's replication ability (p24 of HIV-$1_{V106A/V179D}$ versus HIV-1_{V106A} on day 8; $P < 0.05$).

In the presence of 10 nM EFV, HIV-1_{WT}, HIV-1_{V106I}, and HIV-1_{V106A} failed to propagate and HIV-1_{V179D} exhibited reduced replication compared with that observed in the absence of an NNRTI ($P < 0.01$) (Fig. 2B). HIV-$1_{V106I/V179D}$ and HIV-$1_{V106A/V179D}$ showed efficient replication, though the replication of HIV-$1_{V106A/V179D}$ was slightly reduced compared with that observed in the absence of an NNRTI. In the presence of 100 nM NVP, HIV-1_{WT} and HIV-1_{V106I} failed to propagate and HIV-1_{V179D} exhibited reduced replication compared with that observed in the absence of an NNRTI ($P < 0.01$) (Fig. 2C). HIV-1_{V106A} and HIV-$1_{V106I/V179D}$ showed efficient replication, though the replication of HIV-$1_{V106I/V179D}$ was reduced significantly compared with that observed in the absence of an NNRTI ($P < 0.05$). HIV-$1_{V106A/V179D}$ exhibited replication comparable to that observed in the absence of an NNRTI. In the presence of 10 nM ETV, all of the HIV-1 strains examined exhibited severely compromised replication (Fig. 2D). The results of the replication kinetics experiments were in agreement with the drug susceptibility data.

To analyze the precise roles of V106I and V179D in HIV-$1_{V106I/V179D}$, a competitive HIV-1 replication assay was performed using H9 cells (7, 17). The assay of HIV-1_{V106I} and HIV-$1_{V106I/V179D}$ indicated that the addition of V179D compromised the replication fitness of HIV-1_{V106I} but conferred resistance to EFV and NVP (see Fig. S1A to C in the supplemental material). The assay of HIV-1_{V179D} and HIV-$1_{V106I/V179D}$ indicated that the addition of V106I slightly reduced the replication ability of HIV-1_{V179D} but conferred resistance to EFV and NVP (see Fig. S1D to F in the supplemental material). In the presence of 10 nM ETV, the HIV-1 clones examined could not be passaged efficiently because ETV efficiently suppressed viral replication.

NNRTI susceptibility of HIV-1 clinical isolates. Analysis of the recombinant HIV-1 clones indicated that the combination of V106I and V179D conferred significant resistance to EFV and NVP but not to ETV, although each single mutation did not alter viral susceptibility to NNRTIs (Table 2). To determine the clinical relevance of the results of recombinant HIV-1 analysis, HIV-1 clinical isolates were obtained using MAGIC-5 cells from seven treatment-naïve individuals (cases 1 to 7). In cases 1 and 2, only wild-type amino acids (valine) were detected at the 106th and 179th codons of the HIV-1 RT coding region. In cases 3 and 4, V106I was detected and wild-type valine was found at the 179th codon. In cases 5 and 6, wild-type valine was found at the 106th codon and V179D was identified. In case 7, both V106I and V179D were identified, and none of the other patients harbored both mutations in HIV-1 RT. Subclonal analysis determined that V106I and V179D were on the same virus and that they were highly dominant in case 7 (Table 1). All seven of the patients were infected with HIV-1 subtype B, and no other known resistance-associated mutations were detected at any RT codon other than the 106th and 179th. The six isolates derived from cases 1 to 6 did not show significant resistance to NNRTIs (Table 3). The isolate from case 7, however, exhibited significant resistance to EFV and

TABLE 3. NNRTI susceptibility of clinical HIV-1 isolates

HIV-1 strain (case no.)	Mean EC_{50} (μM) ±SD (fold resistance)[a]		
	EFV	NVP	ETV
Wild type (V106 V179)	0.002 ± 0.0001	0.05 ± 0.004	0.0013 ± 0.0001
V106 V179 isolate (1)	0.002 ± 0.0004 (1.0)	0.04 ± 0.004 (0.8)	0.002 ± 0.0004 (1.5)
V106 V179 isolate (2)	0.002 ± 0.0003 (1.0)	0.04 ± 0.004 (0.8)	0.003 ± 0.0002 (2.3)
V106I V179 isolate (3)	0.002 ± 0.0002 (1.0)	0.03 ± 0.01 (0.6)	0.0012 ± 0.0002 (0.9)
V106I V179 isolate (4)	0.004 ± 0.001 (2.0)	0.09 ± 0.01 (1.8)	0.0024 ± 0.0002 (1.8)
V106 V179D isolate (5)	0.006 ± 0.001 (3.0)	0.07 ± 0.02 (1.4)	0.0015 ± 0.0002 (1.2)
V106 V179D isolate (6)	0.004 ± 0.002 (2.0)	0.07 ± 0.004 (1.4)	0.0011 ± 0.0001 (0.8)
V106I V179D isolate (7)	0.01 ± 0.001 (7.0)	0.19 ± 0.02 (3.8)	0.002 ± 0.0003 (1.5)

[a] The drug susceptibility assay was performed in triplicate and repeated three times (nine experiments). Data are means of nine experiments.

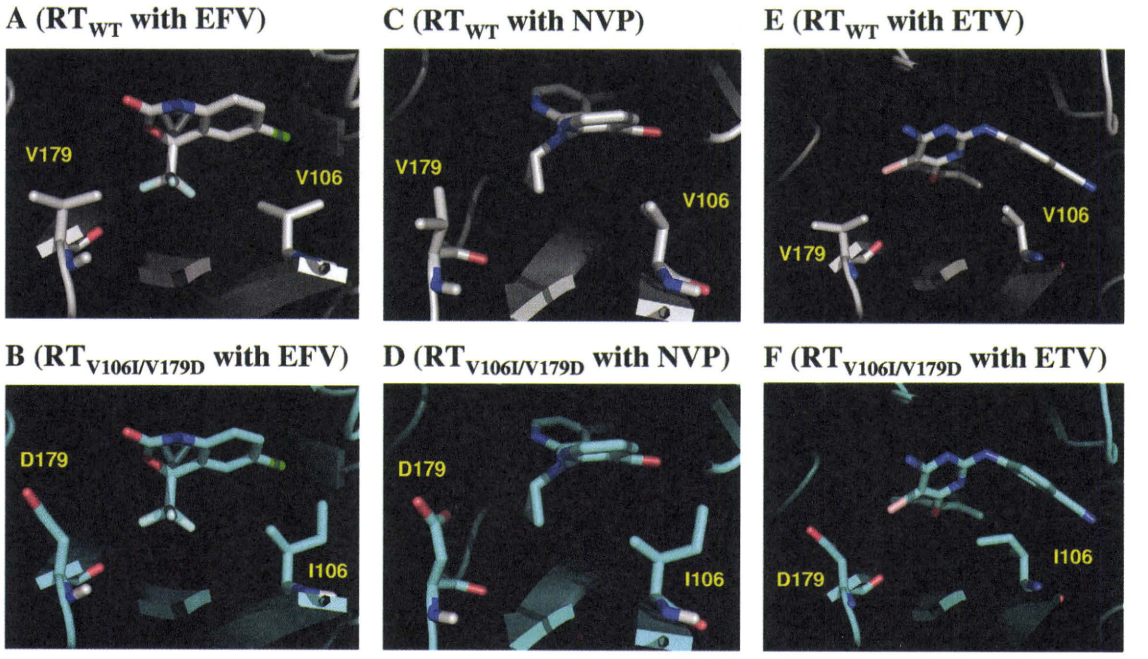

FIG. 3. Interactions of NNRTIs with the 106th and 179th residues of RTs. Interaction sites of NNRTIs and RTs in the models are shown. (A) Wild-type RT (RT_{WT}) with EFV. (B) $RT_{V106I/V179D}$ with EFV. (C) RT_{WT} with NVP. (D) $RT_{V106I/V179D}$ with NVP. (E) RT_{WT} with ETV. (F) $RT_{V106I/V179D}$ with ETV. In the RT_{WT} and $RT_{V106I/V179D}$ models, carbon atoms appear gray and cyan, respectively. NNRTIs and the 106th and 179th residues are highlighted by the stick configuration. Blue sticks, nitrogen; red sticks, oxygen; light blue, fluorine; light green, chlorine; pink sticks, bromine atoms.

NVP but not to ETV. These data confirmed the results obtained by recombinant HIV-1 analysis.

Structural modeling analysis. To obtain structural insight into the molecular mechanisms through which RT mutations alter susceptibility to NNRTIs, we conducted structural analyses by computational methods. A total of 18 structural models of RT-NNRTI complexes were constructed with six RTs (wild-type RT and V179D, V106A, V106I, V106A/V179D, and V106I/V179D mutant RTs) and three NNRTIs (EFV, NVP, and ETV), and the differences in binding energy between the mutant and wild-type complexes ($\Delta\Delta G_b$) were calculated. Notably, $\Delta\Delta G_b$ was proportionally related to the logarithm of fold resistance in RT (Table 2); i.e., the $\Delta\Delta G_b$ values for each RT-NNRTI set were well compatible with the *in vitro* resistance data described above, suggesting that our modeling appropriately reflects the actual mode of binding between the RT molecule and the NNRTI.

In these models, EFV and NVP were predicted to bind to the hydrophobic pocket of RT, as demonstrated in the crystal structures (20, 26). In the wild-type RT, V106 and V179 contributed to the stabilization of the binding of EFV and NVP through hydrophobic interactions (Fig. 3A and C). However, the V106I and V179D mutations attenuated this stabilization by the following mechanisms. In the case of EFV, the V106I mutation caused a steric clash with the chlorine atom on one side of EFV and the V179D mutation caused electrostatic repulsion on the other side of EFV between the carbonyl oxygen atom of EFV and the carboxyl oxygen atoms of D179 in RT (Fig. 3B). In the case of NVP, the V106I mutation caused a steric clash with the aromatic ring of NVP, whereas the V179D mutation reduced hydrophobic contacts with NVP and the charged carboxyl atoms of D179 showed unfavorable contacts with the hydrophobic three-member ring of NVP (Fig. 3D). The effect of a single mutation on binding affinity was relatively moderate because a slight positional shift in EFV and NVP reduced unfavorable contacts. However, V106I V179D double mutations coincidentally caused repulsive interactions at the distinct sites of EFV and NVP which significantly attenuated the affinity of EFV and NVP for RT (Fig. 3B and D).

ETV has rotatable bonds that link aromatic rings. Therefore, it is conceivable that conformational plasticity allowed fine-tuning of ETV conformations for stable binding (Fig. 3E and F). In fact, superposition of the structural models of ETV-RT complexes showed that ETV changed its conformation and position depending on the mutations (Fig. 4A). In contrast, the conformations of EFV and NVP were more rigid due to a lack of rotatable bonds. Therefore, the conformations of EFV and NVP remained similar with various mutant RTs (Fig. 4B and C). These results suggest that the plasticity of the conformation of ETV plays a key role in maintaining its binding affinity for various mutant RTs, as reported in the crystal structural study (4).

DISCUSSION

The results of the present study indicated that the combination of two polymorphic mutations, V106I and V179D, alters the susceptibility of HIV-1 to EFV, as demonstrated in the resistance selection experiments (Fig. 1). Analysis of the recombinant monoclonal HIV-1 strains revealed that the combination confers significant resistance to EFV and NVP but

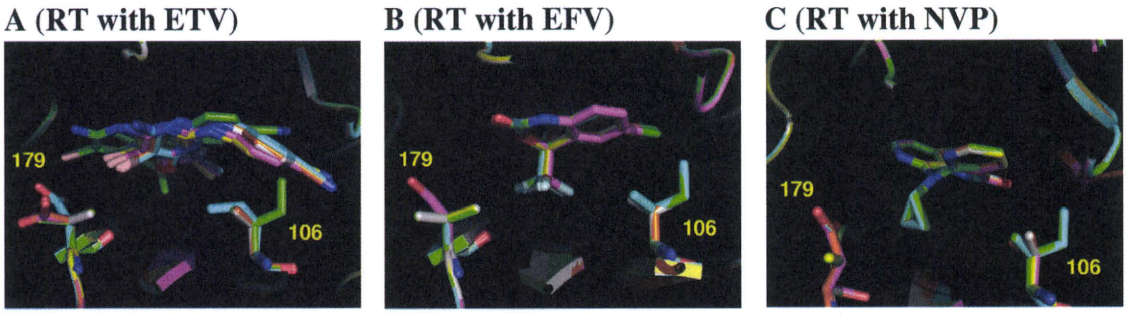

FIG. 4. Superposition of RT_{WT} and five mutant models. (A) RTs with ETV. (B) RTs with EFV. (C) RTs with NVP. NNRTIs and the 106th and 179th residues are highlighted by the stick configuration. White sticks, RT_{WT}; yellow, RT_{V106A}; green, RT_{V106I}; orange, RT_{V179D}; purple, $RT_{V106A/V179D}$; cyan, $RT_{V106I/V179D}$.

not to ETV, although each mutation alone could not alter NNRTI susceptibility (Table 2). Furthermore, one clinical HIV-1 isolate from a treatment-naïve patient who harbored V106I and V179D without any other resistance-associated mutation showed significant resistance to EFV and NVP but not to ETV (Table 3). In a previous study, Tee et al. (29) analyzed HIV-1 RT and protease sequences in 36 antiretroviral-treated patients with detectable viral loads but they could not find any known resistance-associated mutation in 8 patients. In one of their patients on EFV treatment (04MYKL1665), V106I and V179D coexisted in the HIV-1 RT according to GenBank (accession no. AY960901; accessed in October 2009). In a clinical trial of tipranavir, the HIV-1 isolate from one patient (case 48-1084), who experienced NNRTI-treatment failure, harbored V106I and V179D without any other NNRTI resistance-associated mutations (DQ880530) (2). These data strongly indicate that the combination of V106I and V179D also confers significant resistance to NNRTIs *in vivo*.

Structural modeling indicated that V106I and V179D cooperatively reduce NNRTI binding to EFV and NVP. ETV, however, exhibits structural plasticity and can avoid any disturbance caused by the combination of V106I and V179D. This specific structure probably contributes to the efficacy of ETV against many NNRTI-resistant HIV-1 strains, resulting in an excellent rate of response to ETV-containing salvage treatment (18, 21).

Both V106I and V179D are listed as minor ETV resistance-associated mutations in the current version of the IAS-USA Drug Resistance Mutation List (14), but both are not recognized as EFV and NVP resistance-associated mutations. They are often identified individually but rarely coexist in treatment-naïve individuals (Table 1). The combination of V106I and V179D, however, can be found in patients whose baseline HIV-1 held either V106I or V179D after failure of EFV- or NVP-containing treatment (2, 29). Considering that either V106I or V179D was identified in a significant portion of treatment-naïve patients (29/364; 8%) (Table 1), the above information on NNRTI resistance caused by the mutation combination should be recognized by all clinical specialists involved in the interpretation of genotype drug resistance tests and those physicians responsible for changing antiretroviral treatment regimens. In a previous study, we selected EFV-resistant HIV-1 by culture of monoclonal HIV-1 harboring another common polymorphic mutation, K103R ($HIV\text{-}1_{K103R}$), and found the additional emergence of V179D; we then confirmed that the combination of K103R and V179D conferred significant resistance to EFV and NVP (7). Considering these findings together, one assumes that the combinations of polymorphic mutations can reduce NNRTI susceptibility and that other combinations of polymorphic mutations can confer NNRTI resistance. Furthermore, mutations found to be important for one drug may actually have a greater effect on other drugs of the same class. Even polymorphic and minor resistance mutations should be considered carefully when interpreting the results of genotype testing.

ACKNOWLEDGMENTS

This work was supported in part by a Grant-in-Aid for AIDS Research from the Ministry of Health, Labor, and Welfare (H20-AIDS-002) and the Global Center of Excellence Program (Global Education and Research Center Aiming at the Control of AIDS) from the Ministry of Education, Science, Sports and Culture of Japan.

REFERENCES

1. **Bacheler, L. T., E. D. Anton, P. Kudish, D. Baker, J. Bunville, K. Krakowski, L. Bolling, M. Aujay, X. V. Wang, D. Ellis, M. F. Becker, A. L. Lasut, H. J. George, D. R. Spalding, G. Hollis, and K. Abremski.** 2000. Human immunodeficiency virus type 1 mutations selected in patients failing efavirenz combination therapy. Antimicrob. Agents Chemother. **44:**2475–2484.
2. **Baxter, J. D., J. M. Schapiro, C. A. Boucher, V. M. Kohlbrenner, D. B. Hall, J. R. Scherer, and D. L. Mayers.** 2006. Genotypic changes in human immunodeficiency virus type 1 protease associated with reduced susceptibility and virologic response to the protease inhibitor tipranavir. J. Virol. **80:**10794–10801.
3. **Butler, I. F., I. Pandrea, P. A. Marx, and C. Apetrei.** 2007. HIV genetic diversity: biological and public health consequences. Curr. HIV Res. **5:**23–45.
4. **Das, K., A. D. Clark, Jr., P. J. Lewi, J. Heeres, M. R. De Jonge, L. M. Koymans, H. M. Vinkers, F. Daeyaert, D. W. Ludovici, M. J. Kukla, B. De Corte, R. W. Kavash, C. Y. Ho, H. He, M. A. Lichtenstein, K. Andries, R. Pauwels, M. P. De Bethune, P. L. Boyer, P. Clark, S. H. Hughes, P. A. Janssen, and E. Arnold.** 2004. Roles of conformational and positional adaptability in structure-based design of TMC125-R165335 (etravirine) and related non-nucleoside reverse transcriptase inhibitors that are highly potent and effective against wild-type and drug-resistant HIV-1 variants. J. Med. Chem. **47:**2550–2560.
5. **Duan, Y., C. Wu, S. Chowdhury, M. C. Lee, G. Xiong, W. Zhang, R. Yang, P. Cieplak, R. Luo, T. Lee, J. Caldwell, J. Wang, and P. Kollman.** 2003. A point-charged force field for molecular mechanics simulations of proteins based on condensed-phase quantum mechanical calculations. J. Comput. Chem. **24:**1999–2012.
6. **Gatanaga, H., D. Das, Y. Suzuki, D. D. Yeh, K. A. Hussain, A. K. Ghosh, and H. Mitsuya.** 2006. Altered HIV-1 Gag protein interactions with cyclophilin A (CypA) on the acquisition of H219Q and H219P substitutions in the CypA binding loop. J. Biol. Chem. **281:**1241–1250.
7. **Gatanaga, H., A. Hachiya, S. Kimura, and S. Oka.** 2006. Mutations other than 103N in human immunodeficiency virus type 1 reverse transcriptase (RT) emerge from K103R polymorphism under non-nucleoside RT inhibitor pressure. Virology **344:**354–362.

8. **Gatanaga, H., Y. Suzuki, H. Tsang, K. Yoshimura, M. F. Kavlick, K. Nagashima, R. J. Gorelick, S. Mardy, C. Tang, M. F. Summers, and H. Mitsuya.** 2002. Amino acid substitutions in Gag protein at non-cleavage sites are indispensable for the development of a high multitude of HIV-1 resistance against protease inhibitors. J. Biol. Chem. **277:**5952–5961.
9. **Hachiya, A., S. Aizawa-Matsuoka, M. Tanaka, Y. Takahashi, S. Ida, H. Gatanaga, Y. Hirabayashi, A. Kojima, M. Tatsumi, and S. Oka.** 2001. Rapid and simple phenotype assay for drug susceptibility of human immunodeficiency virus type 1 using CCR5-expressing HeLa/CD4(+) cell clone 1-10 (MAGIC-5). Antimicrob. Agents Chemother. **45:**495–501.
10. **Hachiya, A., H. Gatanaga, E. Kodama, M. Ikeuchi, M. Matsuoka, S. Harada, H. Mitsuya, S. Kimura, and S. Oka.** 2004. Novel patterns of nevirapine resistance-associated mutations of human immunodeficiency virus type 1 in treatment-naïve patients. Virology **327:**215–224.
11. **Hachiya, A., E. N. Kodama, S. G. Sarafianos, M. M. Schuckmann, Y. Sakagami, M. Matsuoka, M. Takiguchi, H. Gatanaga, and S. Oka.** 2008. Amino acid mutation N348I in connection subdomain of human immunodeficiency virus type 1 reverse transcriptase confers multiclass resistance to nucleoside and nonnucleoside reverse transcriptase inhibitors. J. Virol. **82:**3261–3270.
12. **Hachiya, A., S. Matsuoka-Aizawa, K. Tsuchiya, H. Gatanaga, S. Kimura, M. Tatsumi, and S. Oka.** 2003. "All-in-One Assay," a direct phenotypic anti-human immunodeficiency virus type 1 drug resistance assay for three-drug combination therapies that takes into consideration in vivo drug concentrations. J. Virol. Methods **111:**43–53.
13. **Holguín, A., and V. Soriano.** 2002. Resistance to antiretroviral agents in individuals with HIV-1 non-B subtypes. HIV Clin. Trials **3:**403–411.
14. **Johnson, V. A., F. Brun-Vezinet, B. Clotet, H. F. Gunthard, D. R. Kuritzkes, D. Pillay, J. M. Scapiro, and D. D. Richman.** 2009. Update of the drug resistance mutations in HIV-1. Top. HIV Med. **17:**138–145.
15. **Kantor, R.** 2006. Impact of HIV-1 pol diversity on drug resistance and its clinical implications. Curr. Opin. Infect. Dis. **19:**594–606.
16. **Kodama, E. I., S. Kohgo, K. Kitano, H. Machida, H. Gatanaga, S. Shigeta, M. Matsuoka, H. Ohrui, and H. Mitsuya.** 2001. 4′-Ethynyl nucleoside analogs: potent inhibitors of multidrug-resistant human immunodeficiency virus variants in vitro. Antimicrob. Agents Chemother. **45:**1539–1546.
17. **Kosalaraksa, P., M. F. Kavlick, V. Maroun, R. Le, and H. Mitsuya.** 1999. Comparative fitness of multi-dideoxynucleoside-resistant human immunodeficiency virus type 1 (HIV-1) in an in vitro competitive HIV-1 replication assay. J. Virol. **73:**5356–5363.
18. **Lazzarin, A., T. Campbell, B. Clotet, M. Johnson, C. Katlama, A. Moll, W. Towner, B. Trottier, M. Peeters, J. Vingerhoets, G. De Smedt, B. Baeten, G. Beets, R. Sinha, B. Woodfall, and the DUET-2 Study Group.** 2007. Efficacy and safety of TMC125 (etravirine) in treatment-experienced HIV-1-infected patients in DUET-2: 24-week results from a randomized, double-blind, placebo-controlled trial. Lancet **370:**39–48.
19. **Lee, M. C., and Y. Duan.** 2004. Distinguish protein decoys by using a scoring function based on a new AMBER force field, short molecular dynamics simulations, and the generalized Born solvent model. Proteins **55:**620–634.
20. **Lindberg, J., S. Sigurdsson, S. Lowgren, H. O. Andersson, C. Sahlberg, R. Noreen, K. Fridborg, H. Zhang, and T. Unge.** 2002. Structural basis for the inhibitory efficacy of efavirenz (DMP-266), MSC194 and PNU142721 towards the HIV-1 RT K103N mutant. Eur. J. Biochem. **269:**1670–1677.
21. **Madruga, J. V., P. Cahn, B. Grinsztejn, R. Haubrich, J. Lalezari, A. Mills, G. Pialoux, T. Wilkin, M. Peeters, J. Vingerhoets, G. De Smedt, L. Leopold, R. Trefiglio, B. Woodfall, and the DUET-1 Study Group.** 2007. Efficacy and safety of TMC125 (etravirine) in treatment-experienced HIV-1-infected patients in DUET-1: 24-week results from a randomized, double-blind, placebo-controlled trial. Lancet **370:**29–38.
22. **Martínez-Cajas, J. L., N. Pant-Pai, M. B. Klein, and M. A. Wainberg.** 2008. Role of genetic diversity amongst HIV-1 non-B subtypes in drug resistance: a systemic review of virologic and biochemical evidence. AIDS Rev. **10:**212–223.
23. **McBurney, S. P., and T. M. Ross.** 2008. Viral sequence diversity: challenges for AIDS vaccine designs. Expert Rev. Vaccines **7:**1405–1417.
24. **Onufriev, A., D. Bashford, and D. A. Case.** 2004. Exploring protein native states and large-scale conformational changes with a modified generalized Born model. Proteins **55:**383–394.
25. **Quan, Y., B. G. Brenner, R. G. Marlink, M. Essex, T. Kurimura, and M. A. Wainberg.** 2003. Drug resistance profiles of recombinant reverse transcriptase from human immunodeficiency virus type 1 subtypes A/E, B, and C. AIDS Res. Hum. Retroviruses **19:**743–753.
26. **Ren, J., R. Esnouf, E. Garman, D. Somers, C. Ross, I. Kerby, J. Keeling, G. Darby, Y. Jones, D. Stuart, and D. Stammers.** 1995. High resolution structures of HIV-1 RT from four RT-inhibitor complexes. Nat. Struct. Biol. **2:**293–302.
27. **Shafer, R. W., and J. M. Schapiro.** 2008. HIV-1 drug resistance mutations: an updated framework for the second decade of HAART. AIDS Rev. **10:**67–84.
28. **Tebit, D. M., I. Nankya, E. J. Arts, and Y. Gao.** 2007. HIV diversity, recombination and disease progression: how does fitness "fit" into the puzzle? AIDS Rev. **9:**75–87.
29. **Tee, K. K., A. Kamarulzaman, and K. P. Ng.** 2006. Prevalence and pattern of drug resistance mutations among antiretroviral-treated HIV-1 patients with suboptimal virological response in Malaysia. Med. Microbiol. Immunol. **195:**107–112.
30. **Wang, J., R. M. Wolf, J. W. Caldwell, P. A. Kollman, and D. A. Case.** 2004. Development and testing of a general amber force field. J. Comput. Chem. **25:**1157–1174.
31. **Yoshimura, K., R. Feldman, E. Kodama, M. F. Kavlick, Y. L. Qiu, J. Zemlicka, and H. Mitsuya.** 1999. In vitro induction of human immunodeficiency virus type 1 variants resistant to phosphoralaninate prodrugs of Z-methylenecyclopropane nucleoside analogues. Antimicrob. Agents Chemother. **43:**2479–2483.

JOURNAL OF VIROLOGY, June 2010, p. 5508–5519 Vol. 84, No. 11
0022-538X/10/$12.00 doi:10.1128/JVI.02483-09

Different *In Vivo* Effects of HIV-1 Immunodominant Epitope-Specific Cytotoxic T Lymphocytes on Selection of Escape Mutant Viruses▽‡

Hirokazu Koizumi,[1]† Masao Hashimoto,[1]† Mamoru Fujiwara,[1] Hayato Murakoshi,[1] Takayuki Chikata,[1] Mohamed Ali Borghan,[1,4] Atsuko Hachiya,[1,3] Yuka Kawashima,[1] Hiroshi Takata,[1] Takamasa Ueno,[1] Shinichi Oka,[2,3] and Masafumi Takiguchi[1]*

Divisions of Viral Immunology[1] and Infectious Disease,[2] Center for AIDS Research, Kumamoto University, 2-2-1 Honjo, Kumamoto 860-0811, and AIDS Clinical Center, International Medical Center of Japan, 1-21-1 Toyama, Shinjuku-ku, Tokyo 162-8655,[3] Japan, and Department of Biological Sciences, College of Arts and Sciences, University of Nizwa, Nizwa, Oman[4]

Received 24 November 2009/Accepted 9 March 2010

HIV-1 escape mutants are well known to be selected by immune pressure via HIV-1-specific cytotoxic T lymphocytes (CTLs) and neutralizing antibodies. The ability of the CTLs to suppress HIV-1 replication is assumed to be associated with the selection of escape mutants from the CTLs. Therefore, we first investigated the correlation between the ability of HLA-A*1101-restricted CTLs recognizing immunodominant epitopes *in vitro* and the selection of escape mutants. The result showed that there was no correlation between the ability of these CTLs to suppress HIV-1 replication *in vitro* and the appearance of escape mutants. The CTLs that had a strong ability to suppress HIV-1 replication *in vitro* but failed to select escape mutants expressed a higher level of PD-1 *in vivo*, whereas those that had a strong ability to suppress HIV-1 replication *in vitro* and selected escape mutants expressed a low level of PD-1. *Ex vivo* analysis of these CTLs revealed that the latter CTLs had a significantly stronger ability to recognize the epitope than the former ones. These results suggest that escape mutations are selected by HIV-1-specific CTLs that have a stronger ability to recognize HIV-1 *in vivo* but not *in vitro*.

HIV-1-specific cytotoxic T lymphocytes (CTLs) have an important role in the control of HIV-1 replication during acute and chronic phases of an HIV-1 infection (5, 28, 33). On the other hand, HIV-1 can escape from the host immune system by various mechanisms. These may include the appearance of HIV-1 carrying escape mutations in its immunodominant CTL epitopes as well as Nef-mediated downregulation of HLA class I molecules. There is a growing body of evidence for the former mechanism, i.e., that CTLs targeting immunodominant HIV-1 epitopes select escape mutants in chronically HIV-1-infected individuals (18, 20, 36), whereas the latter mechanism was proved by demonstrating that HIV-1-specific CTLs fail to kill Nef-positive-HIV-1-infected $CD4^+$ T cells but effectively kill Nef-defective-HIV-1-infected ones or that they suppress the replication of Nef-defective HIV-1 much more than that of Nef-positive HIV-1 (12, 13, 42, 45).

It is speculated that HIV-1 immunodominant epitope-specific CTLs have the ability to suppress HIV-1 replication and effectively select escape mutants. However, the correlation between this ability of the CTLs and the appearance of escape mutants is still unclear, because it is not easy to evaluate the ability of HIV-1-specific CTLs to exert a strong immune pressure *in vivo*. To examine this ability, most previous studies measured the number of HIV-1-specific CTLs or $CD8^+$ T cells and the CTL activity against target cells prepulsed with the epitope peptide or those infected with HIV-1 recombinant vaccinia virus (6, 7, 23, 46). However, the results obtained from such experiments do not reflect the ability of the CTLs to exert immune pressure *in vivo*. We and other groups previously utilized an assay to directly evaluate the ability of the CTLs to suppress HIV-1 replication *in vitro* (1, 17, 18, 42, 43). This assay may be better for evaluation of immune pressure by HIV-1-specific CTLs than other assays, because the ability of the CTLs to suppress HIV-1 replication is directly measured in cultures of HIV-1-infected $CD4^+$ T cells incubated with HIV-1-specific CTL clones. But it still remains unknown whether this assay reflects immune pressure *in vivo*.

In the present study, we investigated whether HIV-1-specific CTLs having a strong ability to suppress HIV-1 replication could positively select escape mutants. Since HLA-A*1101 is known to be an HLA allele relatively associated with a slow progression to AIDS (32), it is speculated that some HLA-A*1101-restricted CTLs would have a strong ability to suppress HIV-1 replication *in vitro*. Therefore, we first focused on 4 well-known HLA-A*1101-restricted CTL epitopes in the present study. We investigated the frequency of CTLs specific for these epitopes in chronically HIV-1-infected individuals, the ability of these CTLs to suppress HIV-1 replication *in vitro*, and whether the escape mutants were selected by the CTLs. Furthermore, we analyzed the expression of Programmed Death-1 (PD-1) on these CTLs *ex vivo* and antigen recognition of them.

* Corresponding author. Mailing address: Division of Viral Immunology, Center for AIDS Research, Kumamoto University, 2-2-1 Honjo, Kumamoto 860-0811, Japan. Phone: 81-96-373-6529. Fax: 81-96-373-6532. E-mail: masafumi@kumamoto-u.ac.jp.

† These authors contributed equally.

‡ Supplemental material for this article may be found at http://jvi.asm.org/.

▽ Published ahead of print on 24 March 2010.

MATERIALS AND METHODS

Patient samples. Informed consent was obtained from all subjects according to the Declaration of Helsinki. For sequence analysis, blood specimens were collected in EDTA. Plasma and peripheral blood mononuclear cells (PBMCs) were separated from heparinized whole blood. Patient HLA type was determined by standard sequence-based genotyping.

Sequence of autologous virus. Viral RNA was extracted from samples of plasma from HIV-1-infected patients by the use of a QIAamp MinElute virus spin kit (Qiagen), and cDNA was synthesized from the RNA with SuperScript RNase H-reverse transcriptase and random primers (Invitrogen). The Nef region and the Gag region were amplified by nested PCR using *Taq* DNA polymerase (Promega). The PCR products were then agarose gel purified and sequenced directly or cloned by use of a TOPO TA cloning kit (Invitrogen). All DNA sequencing was performed by using a BigDye Terminator v1.1 cycle sequencing kit (Applied Biosystems) and an ABI Prism 310 genetic analyzer. The regions of Gag349, Nef73, and Nef84 epitopes were sequenced directly in 124, 121, and 122 individuals, respectively, while those of Nef73 and Nef84 epitopes were sequenced for cloned samples from 10 and 11 individuals, respectively.

Cells. C1R cells expressing HLA-A*1101 (C1R-A*1101) and transporter associated with antigen processing (TAP)-defective RMA-S cells expressing HLA-A*1101 (RMA-S-A*1101) were previously generated and were maintained in RPMI 1640 medium supplemented with 10% fetal calf serum (FCS) and 0.15 mg/ml hygromycin B.

Generation of CTL clones. Peptide-specific CTL clones were generated from an established peptide-specific bulk CTL culture by seeding 0.8 cell/well into U-bottomed 96-well microtiter plates (Nunc, Roskilde, Denmark) together with 200 μl of cloning mixture (RPMI 1640 medium supplemented with 10% FCS and 200 U/ml human recombinant interleukin-2, 5×10^5 irradiated allogeneic PBMC from a healthy individual, and 1×10^5 irradiated C1R-A*1101 cells prepulsed with a 1 μM concentration of the corresponding peptide, Gag349 [ACQGVG GPGHK], Nef73 [QVPLRPMTYK], or Nef84 [AVDLSHFLK]). Wells positive for growth after about 2 weeks were transferred to 48-well plates together with 1 ml of the cloning mixture. The clones were examined for CTL activity by the standard ^{51}Cr release assay. All CTL clones were cultured in RPMI 1640-10% FCS supplemented with 200 U/ml recombinant human interleukin-2 and were stimulated weekly with irradiated target cells prepulsed with the appropriate HIV-1-derived peptide.

HIV-1 clones. Infectious proviral clones of HIV-1, pNL-432, and its Nef mutant, pNL-M20A (containing a substitution of Ala for Met at residue 20 of Nef), reported previously, were used (2). For pNL-432-Nef84-2L9R, the mutation was introduced by site-directed mutagenesis (Invitrogen).

CTL assay for target cells pulsed with HIV-1 peptide. Cytotoxicity activity was measured by the standard ^{51}Cr release assay, as previously described (34). Target cells (2×10^5) were incubated for 60 min with 100 μCi $Na_2{}^{51}CrO_4$ in saline and then washed three times with RPMI 1640 medium containing 10% newborn calf serum (NCS). Labeled target cells (2×10^3/well) were added to 96-well round-bottom microtiter plates (Nunc) along with the appropriate amount of the corresponding peptide. After a 1-h incubation, effector cells were added, and the mixtures were then incubated for 4 h at 37°C. The supernatants were collected and analyzed with a gamma counter.

Intracellular cytokine (ICC) production assay. PBMCs from HLA-A*1101-positive HIV-1-infected patients were stimulated with a given peptide (1 μM) in culture medium (RPMI 1640 medium supplemented with 10% FCS and 200 U/ml recombinant human interleukin-2). After 14 days in culture, the cells were assessed for gamma interferon (IFN-γ) production activity by using a FACSCalibur instrument. Briefly, bulk cultures were stimulated by C1R-A*1101 cells pulsed with or without the corresponding peptide (1 μM) for 2 h at 37°C. Brefeldin A (10 μg/ml) was then added, and the cultures were continued for an additional 4 h. Cells were collected and stained with 7-amino-actinomycin D (7-AAD) at room temperature for 10 min. After 2 washes with RPMI 1640 medium supplemented with 10% FCS, cells were stained with phycoerythrin (PE)-labeled anti-CD8 monoclonal antibody (MAb) (Dako Corporation, Glostrup, Denmark). After having been treated with 4% paraformaldehyde solution, the cells were permeabilized in permeabilization buffer (0.1% saponin and 20% NCS in phosphate-buffered saline) at 4°C for 10 min and stained with fluorescein isothiocyanate (FITC)-labeled anti-IFN-γ MAb (PharMingen, San Diego, CA). After a thorough washing with the permeablization buffer, the cells were analyzed by using the FACSCalibur instrument. Nonspecific binding of anti-IFN-γ MAb and nonspecific production of IFN-γ were excluded by subtracting the data of the negative control, which was the same sample stimulated with C1R-A*1101 cells without the specific peptide and stained with the same MAbs.

For *ex vivo* analysis, PBMCs from HLA-A*1101-positive HIV-1-infected patients were stimulated with the corresponding peptide (1 μM), and IFN-γ production was measured 6 h later, as described above.

HLA class I stabilization assay. The binding of peptides to HLA-A*1101 molecules was tested as previously described (11). RMA-S-A*1101 cells transfected with HLA-A*1101 and human β_2-microglobulin were used. These cells express a very low level of HLA class I molecules on their cell surface when they are cultured at 37°C, whereas empty HLA class I molecules are stably expressed if they are cultured at 26°C. The stabilization of HLA class I molecules is dependent on peptide binding affinity (22, 30, 40). Briefly, RMA-S-A*1101 cells were cultured at 26°C for 14 to 18 h. The cells were incubated at 26°C for 1 h with Nef84 (AVDLSHFLK), Nef84-2L (ALDLSHFLK), or Nef84-2L9R (ALDLSHFLR) peptide at various concentrations and then at 37°C for 3 h. After 2 washes with phosphate-buffered saline (PBS) supplemented with 20% FCS (PBS-20% FCS), they were subsequently incubated for 30 min on ice with an appropriate dilution of MAb TP25.99 (41). After 2 washes with PBS-20% FCS, the cells were incubated for 30 min on ice with an appropriate dilution of FITC-conjugated sheep IgG with anti-mouse Ig specificity (Silenus Laboratories, Hawthorn, Australia). Finally, they were washed three times with PBS-20% FCS, after which the fluorescence intensity was measured by using a flow cytometer (Becton Dickinson, Mountain View, CA).

Surface expression of HLA class I molecules on HIV-1-infected cells. To assess HLA class I expression on HIV-1-infected $CD4^+$ T cells, we stained the cells with anti-HLA-A11 MAb followed by PE-labeled anti-mouse Ig (Pharmingen International, San Diego) and thereafter fixed and permeabilized them for intracellular HIV-1 p24 staining with FITC-labeled anti-p24 MAb KC-57. The expression of HLA class I molecules on HIV-1infected $CD4^+$ T cells was examined by using the FACSCalibur instrument with Cell Quest software (Becton Dickinson, San Jose, CA).

Suppression of HIV-1 replication by HIV-1-specific CTL clones. The ability of HIV-1-specific CTL clones to suppress HIV-1 replication was examined as previously described (42). $CD4^+$ T cells purified by means of anti-human CD4 MAb-coated magnetic beads (MACS beads; Miltenyi Biotec) from PBMCs of an HIV-1-seronegative individual with HLA-A*1101 were cultured and infected with HIV-1 clones. Cultured $CD4^+$ T cells were incubated with an HIV-1 clone for 4 h at 37°C with intermittent agitation and then washed three times with RPMI 1640 medium supplemented with 10% FCS. HIV-1-infected $CD4^+$ T cells were cocultured with an HIV-1-specific CTL clone in culture medium. From day 2 to day 7 postinfection, 10 μl of culture supernatant was collected, and the concentration of p24 antigen (Ag) in the supernatant was measured by conducting an enzyme immunoassay (HIV-1 p24 Ag enzyme-linked immunosorbent assay [ELISA] kit; ZeptoMetrix). Percent suppression was calculated as follows: (concentration of p24 Ag in the supernatant of HIV-1-infected $CD4^+$ T cells cultured with HIV-1-specific CTLs/concentration of p24 Ag in the supernatant of HIV-1-infected $CD4^+$ T cells cultured without the CTLs) × 100.

HLA-peptide tetrameric complexes. The tetrameric complexes of HLA-A*1101, HLA-A*2402, and HLA-A*2601 were synthesized as previously described (3). The purified complexes were enzymatically biotinylated at a BirA recognition sequence located at the C terminus of the heavy chain and were mixed with PE- or allophycocyanin (APC)-conjugated avidin (Molecular Probes) at a molar ratio of 4:1.

Analysis of PD-1 or CD27 CD28 CD45RA expression on HIV-1-specific $CD8^+$ T cells. For the analysis of PD-1 expression, cryopreserved PBMCs of HIV-positive individuals were first stained with Pacific Blue-conjugated CD8 MAb (BD Bioscience) and FITC-conjugated CD3 MAb (Dako Corporation, Glostrup, Denmark) at 4°C for 30 min followed by PE-conjugated PD-1 MAb (BD Bioscience) at the room temperature for 30 min. After 2 washes with RPMI 1640 medium supplemented with 10% FCS, the cells were stained with allophycocyanin (APC)-conjugated tetramer at 37°C for 30 min. After 2 additional washes, the cells were stained with 7-AAD (BD Bioscience) at room temperature for 10 min and analyzed by using flow cytometry (FACS Canto II; BD Bioscience). For the phenotypic analysis of HIV-1-specific $CD8^+$ T cells, the PBMCs were first stained with PE-Cy7-conjugated anti-CD3 (BioLegend), Pacific Blue-conjugated CD8 (BD Bioscience), FITC-conjugated anti-CD27 (BD Bioscience), PE-conjugated anti-CD28 (BioLegend), and phycoerythrin-Texas red (ECD)-conjugated anti-CD45RA (Beckman Coulter) MAbs at 4°C for 30 min. After 2 washes with RPMI 1640 medium supplemented with 10% FCS, the cells were stained with APC-conjugated tetramer at 37°C for 30 min. After 2 additional washes, the cells were stained with 7-AAD at room temperature for 10 min and analyzed by using flow cytometry.

Enzyme-linked immunospot (ELISPOT) assay. Cryopreserved PBMCs of 2 HLA-A*1101$^+$ HIV-1-infected individuals (KI-015 and KI-036) were plated out in 96-well polyvinylidene plates (Millipore, Bedford, MA) which had been pre-

coated with 0.5 μg/ml anti-IFN-γ MAb 1-DIK (Matbech, Stockholm, Sweden). The appropriate amount of Nef73 or Nef84 peptides was added in a volume of 50 μl, and then PBMCs were added at 1×10^5 cells/well in a volume of 100 μl. The plate was incubated for 40 h at 37°C in 5% CO_2 and was washed with PBS before the addition of biotinylated anti-IFN-γ MAb (Mabtech) at 0.5 μg/ml. After it was incubated at room temperataure for 100 min and then washed with PBS, streptavidin-conjugated alkaline phospatase (Mabtech) was added following a 40-min incubation at room temperature. Individual cytokine-producing cells were detected as dark spots after a 20-min reaction with 5-bromo-4-chloro-3-indolyl phosphate and Nitro Blue Tetrazolium by using an alkaline phosphatase-conjugated substrate (Bio-Rad, Richmond, CA). The spot number was counted by using an Eliphoto counter (Minerva Teck, Tokyo, Japan). The number of spots for each peptide-specific T cell response was caluculated by subtracting the negative-control spots.

RESULTS

Immunodominancy of 4 HLA-A*1101-restricted HIV-1 epitopes. We first focused on HIV-1 CTL epitopes presented by only a given HLA allele that influences the control of HIV-1, because the effect of each epitope presented by the same HLA class I allele on the ability of specific CTLs to suppress HIV-1 replication and to select escape mutants can be compared. HLA-A*1101 is an HLA allele relatively associated with a slow progression to AIDS (32), implying that some epitope-specific CTLs may have the ability to suppress HIV-1 replication. We selected 4 out of many known HLA-A*1101-restricted HIV-1 epitopes (Gag349, ACQGVGGPGHK; Pol675, QIIEQLIKK; Nef73, QVPLRPMTYK; and Nef84, AVDLSHFLK; or Nef84-2L, ALDLSHFLK [both sequences are frequently found in clade B]), because CTLs specific for these epitopes were previously shown to be frequently detected in chronically HIV-1-infected individuals (10, 14, 19). We re-evaluated whether $CD8^+$ T cells specific for these HIV epitopes could be frequently detected in chronically HIV-1-infected Japanese individuals carrying HLA-A*1101. PBMC from these individuals and HIV-1-seronegative HLA-$A*1101^+$ individuals were stimulated with these epitope peptides and cultured for 2 weeks. The percentage of specific $CD8^+$ T cells in these cultures was determined by performing an intracellular cytokine (ICC) production assay using these epitope peptides (Fig. 1A). Pol675-specific $CD8^+$ T cells were detected in only 1 of the 8 individuals, whereas Gag349-specific, Nef73-specific, and Nef84- or Nef84-2L-specific ones were detected in 12 of 16 individuals, 13 of 16 individuals, and 11 of 16 individuals, respectively (Fig. 1B). These results indicate that Gag349, Nef73, and Nef84 (or Nef84-2L) are recognized as immunodominant epitopes in HIV-1-infected Japanese individuals carrying HLA-A*1101. We therefore focused on these 3 epitopes for further studies.

Ability of 3 HLA-A*1101-restricted HIV-1-specific CTLs to suppress HIV-1 replication *in vitro*. To investigate the ability of these T cells to suppress HIV-1 replication, we next established 5 Gag349-specific, 7 Nef73-specific, and 3 Nef84-specific CTL clones from PBMC of chronically HIV-1-infected individuals carrying HLA-A*1101. These CTL clones exhibited a strong cytolytic activity against C1R-A*1101 cells prepulsed with the corresponding epitope peptide (Fig. 2A) and against those infected with recombinant vaccinia virus expressing the HIV-1 SF2 Nef or Gag protein (data not shown). We investigated the ability of these CTL clones to suppress HIV-1 replication in primary $CD4^+$ T cells infected with the NL-432 clone or its Nef mutant NL-M20A, which has the ability to downregulate the cell surface expression of CD4 but not that of HLA-class I A and B molecules, in HIV-1-infected cells (2). Indeed, NL-432-infected $CD4^+$ T cells exhibited the downregulation of HLA-A*1101, whereas NL-M20A-infected ones did not (Fig. 2B). Both Nef73-specific and Nef84-specific CTL clones completely suppressed the replication of both NL-432 and NL-M20A at effector/target cell (E:T) ratios of 1:1 and 0.1:1 (Fig. 2C). A Gag349-specific CTL clone partially suppressed NL-432 replication and completely suppressed that of NL-M20A at an E:T ratio of 1:1 but failed to suppress the replication of either clone at an E:T ratio of 0.1:1 (Fig. 2C). Analysis using 6 Gag349-specific, 7 Nef73-specific, and 3 Nef84-specific CTL clones confirmed that the ability of the Nef73-specific and Nef84-specific CTL clones to suppress HIV-1 replication was much stronger that of the Gag349-specific ones (Fig. 2D). It also revealed that Nef-mediated HLA-class I downregulation did not affect the recognition of HIV-1-infected $CD4^+$ T cells by Nef73-specific and Nef84-specific clones. These results together indicate that Nef73-specific and Nef84-specific CTLs have a strong ability to suppress HIV-1 replication *in vitro*.

***Ex vivo* analysis of Nef73-specific and Nef84-specific CTLs in chronically HIV-1-infected individuals.** Nef73-specific and Nef84-specific CTLs could be induced from the memory T-cell pool by *in vitro* stimulation with the specific peptides in more than 50% of chronically HIV-1 infected individuals carrying HLA-A*1101 (Fig. 1). To clarify whether these specific T cells would be elicited *in vivo*, we analyzed PBMCs from chronically HIV-1-infected individuals carrying HLA-A*1101 by using the specific tetramers. Nef73-specific $CD8^+$ T cells were detected for 16 of 20 chronically HIV-1-infected HLA-$A*1101^+$ individuals, and Nef84-specific $CD8^+$ T cells were detected for 13 of 17 (Fig. 3). These results together with those shown in Fig. 1 indicate that both Nef73-specific and Nef84-specific CTLs were effectively elicited in chronically HIV-1-infected HLA-$A*1101^+$ individuals.

Association of an HLA-A*1101 allele with mutations in the 3 CTL epitopes. We speculated that these 2 Nef epitope-specific CTLs having a strong ability to suppress HIV-1 replication could select escape mutants but that Gag349-specific CTLs having a weak ability to suppress HIV-1 replication could not. We therefore analyzed the sequences of these epitopes and their flanking regions from HLA-$A*1101^+$ and HLA-$A*1101^-$ individuals who had been chronically infected with HIV-1 to clarify whether they selected the escape mutations. In the Gag349 epitope, only the 9S mutation was found, but there was no significant difference in the frequency of this mutation between the HLA-A*1101-positive and -negative individuals (Fig. 4A). In the Nef73 epitope, several mutations were found at positions 2, 4, 5, 8, 9, and 10 (Fig. 4B). The 9F mutation was frequently found, but there was no significant difference in the frequency of this mutation, nor in that of the other mutations, between the HLA-A*1101-positive and -negative subjects. In the Nef84 epiope, there were several mutations, at positions 2, 3, 5, 6, 7, 8, and 9, though the mutations at positions 2, 6, and 9 were the most frequently detected ones (Fig. 4C). The frequency of the Arg mutation at position 9 was significantly higher in HLA-A*1101-positive individuals than in HLA-A*1101-negative ones ($P < 0.0001$) (Fig. 4C). In contrast, the mutations at position 2 were significantly more fre-

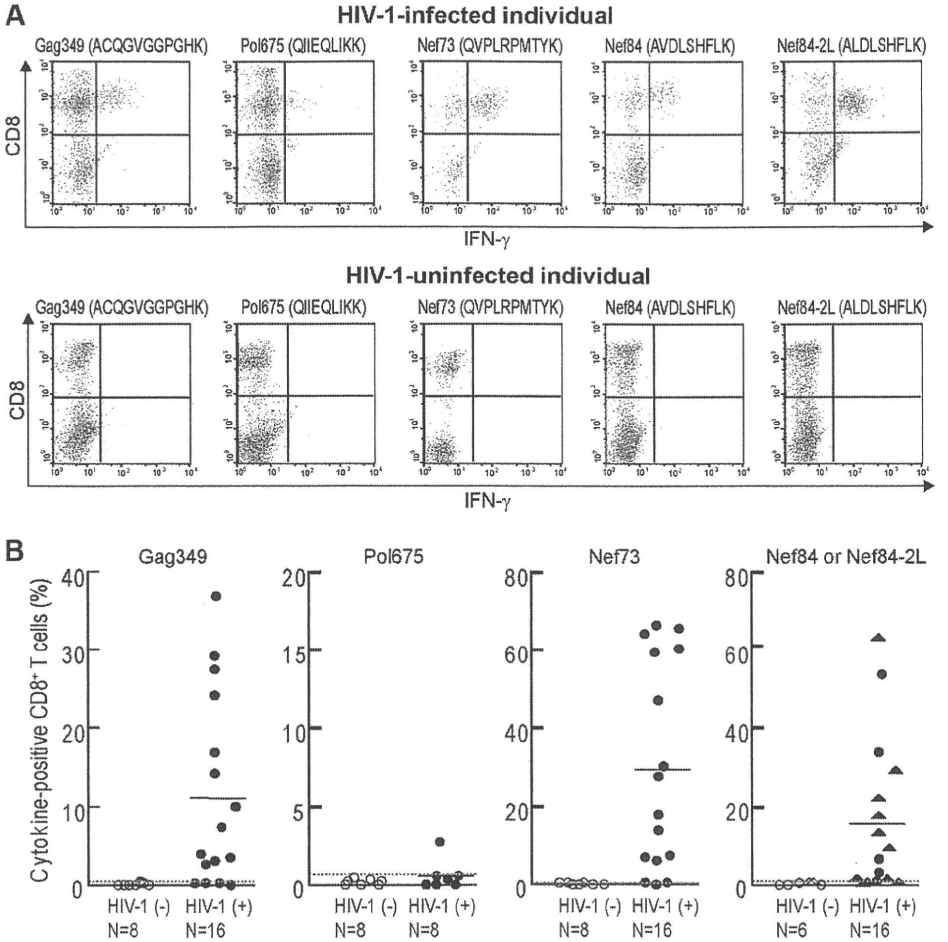

FIG. 1. Four HLA-A*1101-restricted HIV-1-specific $CD8^+$ T cells in chronically HIV-1-infected HLA-$A*1101^+$ individuals. (A) After PBMC from an HLA-$A*1101^+$ HIV-1-infected and HIV-1-uninfected individuals had been stimulated singly with each of the indicated peptides for 2 weeks, HIV-1-specific $CD8^+$ T cells were detected by measuring IFN-γ-producing $CD8^+$ T cells in the culture after stimulation with the corresponding peptide-pulsed cells. Either Nef84 or Nef84-2L peptide was used for individuals infected with HIV carrying the corresponding sequence. A representative result is shown. (B) Summary of ICC assays for HLA-$A*1101^+$ HIV-1-infected individuals and HIV-1-uninfected individuals. For detection of Nef84- and Nef84-2L-specific $CD8^+$ T cells, Nef84 and Nef84-2L peptides were incubated with cells from individuals infected with the wild type or the 2F and 2L viruses, respectively. The circle symbols and the triangle symbols represent the frequency of IFN-γ-producing $CD8^+$ T cells after stimulation with Nef84 and Nef84-2L peptides, respectively. The average + 3 SD of IFN-γ-producing $CD8^+$ T cells in HIV-1-uninfected individuals was defined as a positive value (Gag349, >0.34%; Pol675, >0.56%; Nef73, >0.32%; Nef84 or Nef84-2L, >0.63%). Dotted lines indicate the average + 3 SD, and solid lines indicate the average in HIV-1-infected individuals.

quently detected for HLA-A*1101-negative individuals than for HLA-A*1101-positive ones ($P = 0.045$), suggesting that they were not selected by HLA-A*1101-restricted CTLs. There were 3 mutations (Phe, Tyr, and Arg) at position 6. The frequency of each one at position 6 was not significantly higher for HLA-A*1101-positive individuals than for HLA-A*1101-negative ones. These results together suggest that only the 9R mutation was selected by Nef84-specific CTLs.

There were several mutations in the flanking region of these epitopes, but no significant difference in them between the HLA-A*1101-positive and -negative individuals was found (data not shown).

In vitro recognition of the 9R mutation by Nef84-specific CTLs. We speculated that the 9R mutant is an escape mutant from Nef84-specific CTLs because this mutation is associated with the HLA-A*1101 allele. We therefore investigated whether or not the Nef84-specific CTLs could recognize the Nef84-9R mutant epitope. We first tested the activity of Nef84-specific CTL clones in killing target cells prepulsed with the Nef84-9R mutant peptide. Three Nef84-specific CTL clones effectively killed target cells prepulsed with Nef84 or Nef84-2L wild-type peptide but failed to kill those prepulsed with Nef84-2L9R peptides (Fig. 5A). The results of an HLA class I stabilization assay showed that the affinity of the Nef84-2L9R peptide for HLA-A*1101 was much weaker than that of Nef84 or Nef84-2L for it (Fig. 5B). Taken together, these results suggest that the Nef84-2L9R peptide is very weakly presented in HIV-1 mutant virus-infected cells because of the very low affinity of Nef84-2L9R peptide for HLA-A*1101. We generated an NL-432 mutant carrying 2L and 9R mutations of Nef84 (NL-432-Nef84-2L9R) virus and infected HLA-$A*1101^+$ $CD4^+$ T cells with this virus. The infected cells showed down-

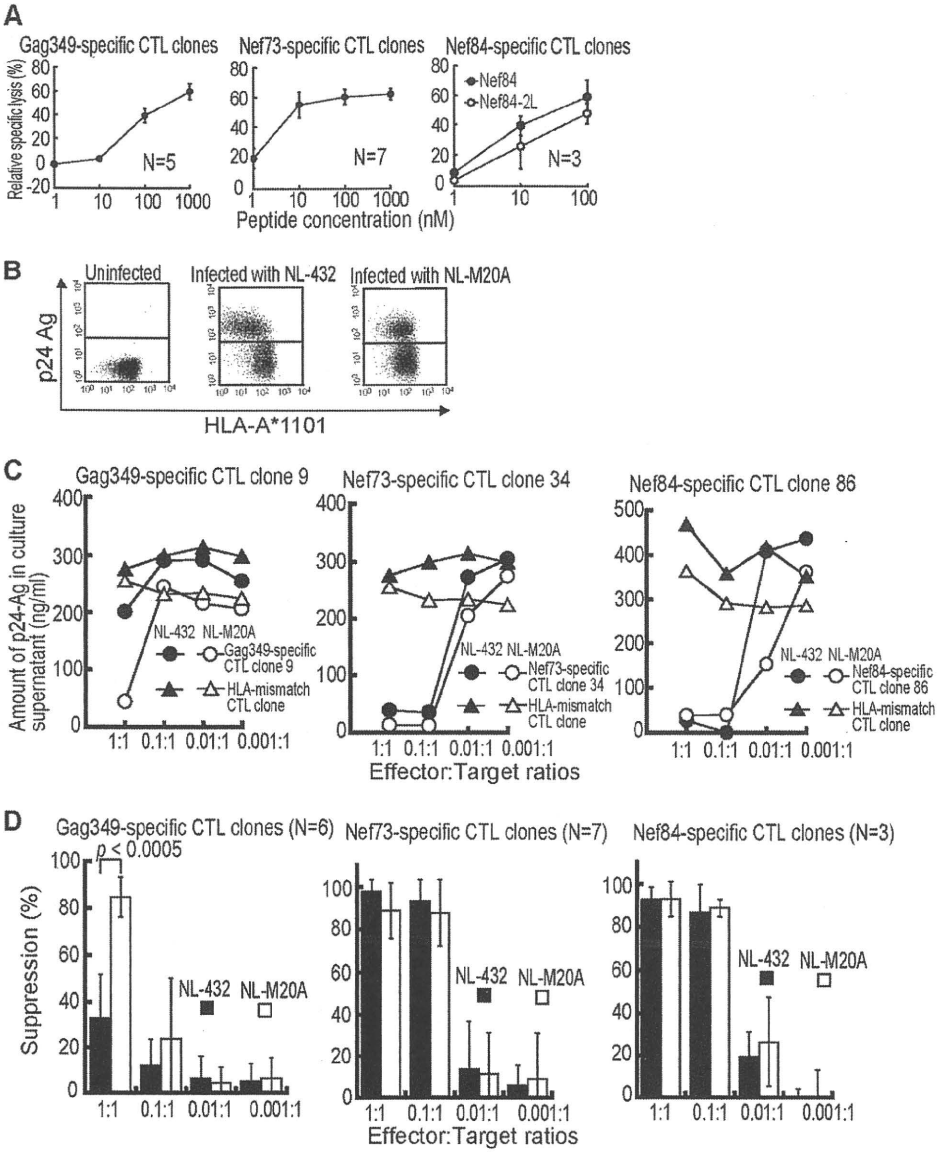

FIG. 2. Ability of HLA-A*1101-restricted CTLs to suppress HIV-1 replication in HIV-1-infected $CD4^+$ T cells. (A) Cytolytic activities of HLA-A*1101-restricted HIV-1-specific CTLs (5 Gag349-specific, 7 Nef73-specific, and 3 Nef84 consensus B-specific CTL clones) were tested by using C1R-A*1101 cells pulsed with various concentrations of the corresponding peptide (effector-to-target-cell ratio = 2:1). (B) Surface expression of HLA class I molecules on $CD4^+$ T cells infected with HIV-1 NL-432 or NL-M20A. $CD4^+$ T cells infected with HIV-1 NL-432 or NL-M20A were stained with anti-HLA-A*1101 and anti-p24 MAbs and then analyzed by using flow cytometry. (C) Ability of HLA-A*1101-restricted CTLs to suppress HIV-1 replication in cultures of HIV-1-infected $CD4^+$ T cells. $CD4^+$ T cells from an HLA-A*1101^+ healthy individual were infected with NL-432 or NL-M20A and then cocultured with HLA-A*1101-restricted CTL clones or HLA-mismatch CTL clone (HLA-B*5101) at various effector-to-target ratios. HIV-1 p24 Ags in the supernatant were measured on day 6 or 7 postinfection by conducting an enzyme immunoassay. (D) Analysis using multiple HLA-A*1101-restricted CTLs to suppress replication of NL-432 or NL-M20A.

regulation of HLA-A*1101 on target cells infected with NL-432 or NL-432-Nef84-2L9R but not on those infected with NL-M20A (Fig. 5C). Thus, these result also revealed that the 2L9R mutations do not affect the downregulation of HLA class I molecules. Three Nef84-specific CTL clones failed to suppress replication of NL-432-Nef84-2L9R (Fig. 5D), whereas these T-cell clones effectively suppressed replication of NL-432 at E:T ratios of 1:1 and 0.1:1 (Fig. 5D and 5E). These results indicate that the CTL clones could not recognize cells infected with NL-432-Nef84-2L9R and confirmed 9R to be an escape mutation.

Different surface expression levelS of PD-1 between Nef73-specific and Nef84-specific CTLs. Both Nef73-specific and Nef84-specific CTL clones effectively suppressed HIV-1 replication *in vitro*. In contrast, the latter CTLs selected an escape mutation *in vivo*, whereas the former ones did not. These findings suggest the possibility that Nef73-specific CTLs cannot mediate selection of escape mutants *in vivo*. PD-1 expression

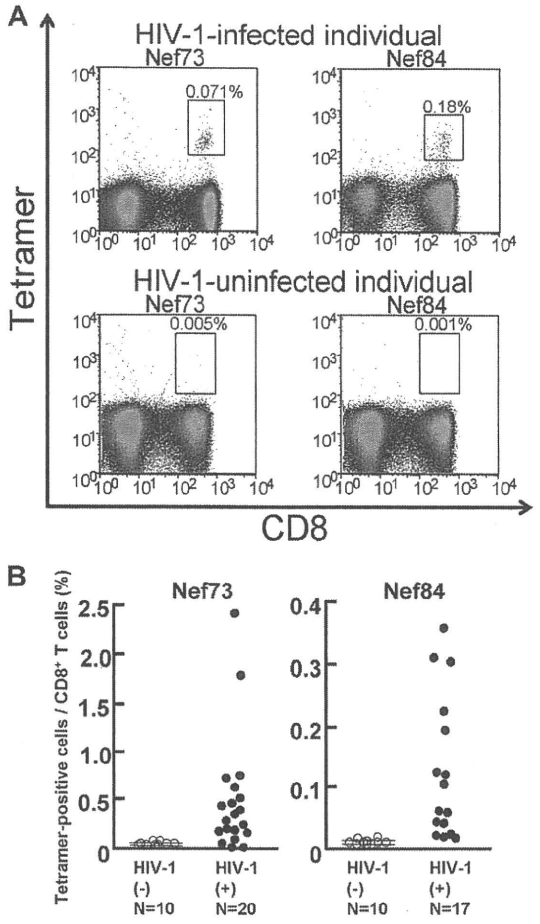

FIG. 3. Frequency of HLA-A*1101-restricted Nef epitope-specific $CD8^+$ T cells. PBMCs from HLA-A*1101^+ HIV-1-infected or HIV-1-uninfected individuals were examined by using Nef73-specific or Nef84-specific tetramers and anti-CD8 MAb or by using only anti-CD8 MAb. (A) A representative result of Nef73-specific or Nef84-specific tetramer binding $CD8^+$ T cells. (B) Summary of frequency of HLA-A*1101^+-restriced Nef73-specific or Nef84-specific $CD8^+$ T cells in HIV-1-infected individuals and HIV-1-uninfected individuals. The mean frequencies + 3 SD of Nef73-specific and Nef83-specific $CD8^+$ T cells among total $CD8^+$ T cells from the HIV-1-uninfected individuals were 0.032% + 0.045% and 0.009% + 0.012%, respectively. More than 0.077% and 0.021% were evaluated as showing positive binding of Nef73-specific and Nef84-specific tetramers, respectively.

on HIV-1-specific T cells is known to be associated with dysfunction of T cells (15, 35, 44, 47). Therefore, high expression of PD-1 on the CTL surface is a possible reason why Nef73-specific CTLs failed to select escape mutants. To clarify the PD-1 expression on Nef73-specific and Nef84-specific CTLs, we stained PBMCs from HLA-A*1101^+ HIV-1-infected individuals with anti-PD-1 and anti-CD8 MAbs aND with the specific tetramer (Fig. 6A and B). Nef73-specific and Nef84-specific $CD8^+$ T cells were, respectively, detected by the tetramers in 16 and 13 chronically HIV-1-infected individuals carrying HLA-A*1101 (Fig. 3), but only 15 and 8 individuals had a sufficient number of Nef73-specific and Nef84-specific $CD8^+$ T cells for analysis of PD-1 expression, respectively. The Nef73-specific $CD8^+$ T cells expressed a significantly higher level of PD-1 than the Nef84-specific ones (Fig. 6C). But only 8 individuals (2 having the 9R mutant and 6 having wild-type Nef84) had enough Nef84-specific $CD8^+$ T cells for analysis of PD-1 expression. We did not find any difference in the expression levels of PD-1 between these 2 groups (see Fig. S1 in the supplemental material). These results suggest that the 9R mutation did not influence the level of PD-1 on Nef84-specific $CD8^+$ T cells.

Both Nef84- and Nef73-specific CTLs, enough for the analysis of PD-1 expression, were detected in only 5 of the individuals tested. We compared the levels of PD-1 between the CTLs within the same individual. A similar difference was found between these CTLs within each individual (Fig. 6D). PD-1 is known to be upregulated on activated T cells (34). Therefore, we speculate that Nef84-specific CTLs are not activated, because the wild-type virus disappeared and the Nef84-9R escape mutant was selected in many HLA-A*1101^+ individuals, resulting in downregulation of PD-1 expression on the T cells. We investigated the sequences of these Nef epitopes in HIV-1 from the 5 individuals whose Nef73-specific and Nef84-specific $CD8^+$ T cells were analyzed for PD-1 expression. These 5 individuals were infected with HIV-1 carrying the wild-type Nef73 sequence, whereas the sequence of Nef84 was wild type (2V or 2L) in 3 of these individuals, Nef84-9R in 1, and a mixture of both in 1 individual (Table 1). The Nef84-specific $CD8^+$ T cells from the individual infected with the Nef84-9R mutant (KI-390) expressed the highest level of PD-1 among the T cells from these 5 individuals (Fig. 6D). Together with the results showing no difference in the expression levels of PD-1 between individuals infected with the 9R mutant and those infected with the wild-type virus, these results exclude the possibility that the lower level of expression of PD-1 on Nef84-specific T cells resulted from the appearance of the Nef84-9R mutant virus in these individuals.

A recent study showed that PD-1 is highly expressed on effector memory T cells and that its expression is related to the differentiation of $CD8^+$ T cells (37). Therefore, the difference in expression of PD-1 may result from the difference in differentiation status between these 2 Nef epitope-specific T cells. We analyzed the CD27 CD28 CD45RA phenotype of these T cells in the 5 individuals to clarify differentiation of the T cells. The results showed no difference in differentiation status between these 2 Nef epitope-specific T cells, although effector and late effector subsets were predominantly detected in Nef84-specific and Nef73-specific T cells from one individual (see Fig. S2 in the supplemental material). These results indicate that a difference in expression of PD-1 between these T cells was not due to the difference in differentiation status.

We speculate that there is no difference in the level of PD-1 expression between Nef73-specific and Nef84-specific CTL clones, because both CTL clones showed strong ability to suppress HIV-1 replication. To complement the *ex vivo* data, we analyzed the PD-1 expression on our *in vitro*-generated CTL clones. The results showed that both CTL clones expressed a low level of PD-1 and that there was no difference in the expression level between these CTL clones (data not shown).

We further investigated PD-1 expression on 2 CTLs having a strong ability to suppress HIV-1 replication. HLA-A*2402-restricted Nef138-specific CTLs were recently shown to have a strong ability to suppress HIV-1 replication and to select

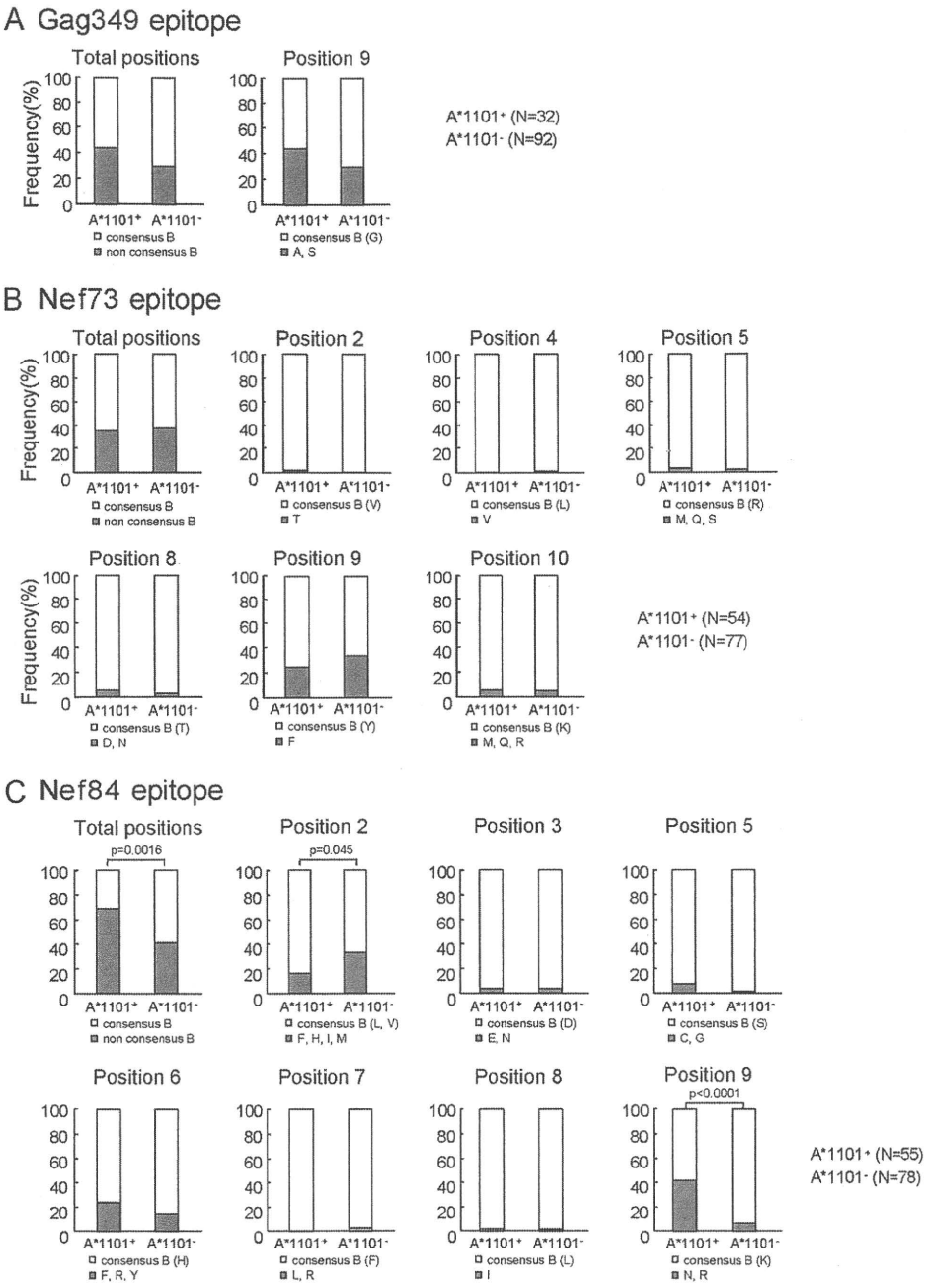

FIG. 4. Frequency of mutations in 3 HLA-A*1101-restricted epitopes. Three epitope sequences, Gag349 (A), Nef73 (B), and Nef84 (C), from HLA-A*1101-positive and HLA-A*1101-negative individuals chronically infected with HIV-1 were analyzed. Consensus sequences of these epitopes in clade B are as follow: Gag349, ACQGVGGPGHK; Nef73, QVPLRPMTYK; Nef84, AVDLSHFLK and ALDLSHFLK. The frequency of mutations in the total sequence of the epitopes was calculated as (number of individuals having the mutation[s]/number of individuals tested) × 100, whereas those at a given position were calculated as (number of individuals having the mutation[s] at a given position/number of individuals tested) × 100. The results were compared between HLA-A*1101-positive and HLA-A*1101-negative individuals, and the *P* values were determined by using Fisher's exact test.

Nef138-2F escape mutants (18). HLA-A*26-restricted Gag169-specific $CD8^+$ T cells also have a strong ability to suppress HIV-1 replication but cannot select any escape mutant (unpublished observation). PD-1 expression on Nef138-specific and Gag169-specific $CD8^+$ T cells from chronically HIV-1-infected individuals was measured by using specific tetramers and anti-PD-1 MAbs. PD-1 expression on Nef138-specific $CD8^+$ T cells was lower than that on the Gag169-specific ones. Taken together, these results show that PD-1 expression on $CD8^+$ T cells that can select escape mutants is significantly lower than that on $CD8^+$ T cells that are unable to select escape mutants (Fig. 6E).